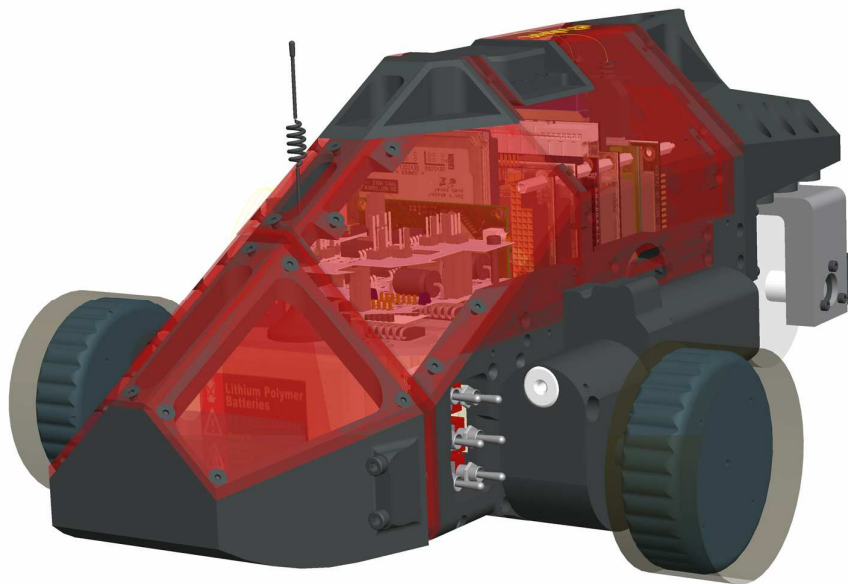




## **A Second-Generation NDE Inspection Robot**

---



**University of Cape Town**  
Department of Mechanical Engineering

Ian Alan Baldwin 2006

---

## **DECLARATION**

---

This thesis is submitted in complete fulfilment of a M.Sc. (Eng) (Mechanical Engineering) at the University of Cape Town.

I know the meaning of plagiarism and declare that all the work in the document, save for that which is properly acknowledged, is my own. Each contribution to, and quotation in, this thesis from the work(s) of other people has been attributed, and has been cited and referenced.

I have not allowed, and will not allow, anyone to copy my work with the intention of passing it off as his or her own work.

Signature:

**IAN ALAN BALDWIN**

Date:

**19<sup>TH</sup> JANUARY, 2007**

---

## SUMMARY

---

### BACKGROUND

Since the early 1950's, **Non-Destructive Evaluation** (NDE) has been revolutionizing all fields of industry but particularly production and maintenance. For the manufacturing sector, the widespread implementation of accurate NDE techniques (such as ultrasonic inspection) as well as the introduction of fracture mechanics, allowed engineers to more accurately predict the lifetime of components before failure [1], leading to an increased rejection in faulty or sub-standard components.

A similar revolution took place in sectors involved with maintenance and inspection. Flaw detection would enable technicians to establish whether failure was imminent, improving safety and preventing scenes as shown in **Figure (A) 1** below:



FIGURE (A) 1: *PRESTIGE* SINKING

This unfortunate photograph is of the Liberian-owned *Prestige* sinking off of the Spanish *Costa de la Muerte* (Death Coast) in late 2002[5]. The *Prestige* was bound for Singapore and carrying 77 000 tonnes of crude oil, and the resulting slick had enormous environmental, social and economic impacts on the region. Better and more rigorous inspection procedures may have prevented the *Prestige*'s cataclysmic failure.

### ROBOTICS & NDE

Inspection of marine vessels in dry-dock can be a hazardous job. Manual NDE techniques require technicians to make use of scaffolding and gantries to be able to gain access to all sections of a ship's hull, which in some cases may be in excess of six stories off of the dry-dock floor. It is also time consuming; in the example of a medium-sized grain carrier, it may take technicians several months to fully inspect the hull and certify the vessel seaworthy.

Shown overleaf in **Figure (A) 2** is a typical setup at the Robertson Dry Dock in Cape Town:



FIGURE (A) 2: MANUAL INSPECTION

Visible in the image is the scaffolding the technicians use to gain access to the extremities of the hulls. Working on a platform which can be in excess of eighteen metres off the dry-dock floor poses a serious accident risk to personnel. Use of a **R**emotely **O**perated **V**ehicle (**ROV**) would eliminate risk to NDE personnel while potentially being able to reduce overall inspection time.

As a result of the growth of robotics as an industry, increasingly more systems are being developed that are capable of conducting NDE inspection. Robotics inspection systems reduce the risk to technicians, and are capable of performing a variety of inspection procedures.



FIGURE (A) 3: REFINERY 'BOTS

**Figure (A) 3** shows two robots development for use in petroleum and petrochemical environments. *Neptune*, on the left, is a petroleum-storage inspection vehicle [16], equipped with a payload consisting of video cameras and **U**ltrasonic **T**esting (**UT**) equipment. The adjacent frame show the Explorer II [17], a vehicle designed for pipe inspection in a live-gas environment. While these platforms are well-suited to their designed task, they do not adapt well to marine inspection.

#### **PREVIOUS DEVELOPMENT**

Development of a dedicated NDE capable robot was the subject of a 2004 conjoint undergraduate thesis project [26] [27]. Shown in **Figure (A) 4** overleaf is the end result of the project, dubbed *Pinky*:



## EROBOT

An Industrial NDE robot



FIGURE (A) 4: PREVIOUS NDEBOT

As a first-generation prototype *Pinky* performed adequately; however in order to produce a platform that would be capable of performing in an industrial environment major improvements had to be made to the concept. These included ruggedization of the platform, expansion of the NDE techniques used as well as cost evaluation of the platform, as a whole, to ensure market competitiveness.

This project took the experiences gained from the first NDE prototype and incorporated them into the next generation NDEbot.

### **EROBOT: 2ND GENERATION NDEBOT**



FIGURE (A) 5: eROBOT TRAVELLING ON A VERTICAL WALL

**eRobot** is a 2<sup>nd</sup> generation inspection robot fusing the power of modern embedded computing technology with the diversity of low-cost robotics. Although primarily designed for the inspection of marine vessels in dry-dock, eRobot makes use of a highly modular design in order to be able to fulfil a variety of inspection tasks. Custom-sintered magnets and custom made drive-units allow eRobot to adhere to ferro-magnetic structures and to travel inverted if required.

Communication is realised over a standard wireless (**WiFi**) network and utilises a standard LAN architecture to provide full internet connectivity, allowing the logging of

position and data to its associated server and website. Control of the robot is made possible by a standard joystick and laptop, giving the operator full and intuitive control of the vehicle. An embedded computer running open-source software and utilising custom communication and control programs ensures a rapid and accurate response to any user-input. Making use of **Differential Global Positioning System (DGPS)** technology, eRobot is capable of downloading correctional data from its associated DGPS server, allowing for accurate 3-dimensional positioning.

**EROBOT: CAPABILITIES**

	<b>SPECIFICATION</b>	<b>DESCRIPTION</b>
<b>Physical</b>	Straight line speed	0.2 m/s
	Manoeuvrability	Full manoeuvrability with sufficient adherence to travel inverted.
	Operating Range	Operating range of over 30 metres
	Operating Cycle	Continuous operation for a 2 hour period.
	Multiple Payloads	Capacity to accommodate a variety of NDE techniques
	Modular Design	Allow for incorporation of alternate drive or sensor modules.
	Weight	Weight of 8 kilograms allows one-person operation.
	Profile	Profile allows travel in standard 14" piping.
<b>Control &amp; Interface</b>	Human Interface	Basic user interface with minimal learning or training.
	Expandability	Capacity for future implementation of self - navigation and environmental awareness
	Data Acquisition	GPS enabled to allow co-ordinate mapping
	Media Feed	Capacity for real-time video streaming
<b>Other</b>	Commercially competitive	Economically competitive with equivalent market-available platforms.
	Expansion & Upgradeability	Embedded computing allows for future development of more advanced capabilities.

TABLE (A) 1: CAPABILITIES

**CONCLUSIONS & RECOMMENDATIONS**

In conclusion, the base performance of the robot was acceptable. Although the vehicle is not ready for the rigours of an industrial setting, it provided a useful prototype to test the validity of the concept itself as well as other concepts (navigation, networking and so on). The main performance criteria of the system are analysed below and recommendations are made for future development work on the vehicle.

**MECHANICAL DESIGN**

Design of the robot in a modular fashion allowed for the simple assembly/disassembly for frequent modifications, and was considered a success. Structurally the robot was sound, and showed no sign of wear at the end of the project. However, reduction in the **weight** of the robot chassis by re-designing the vehicle with an **aluminium chassis** would benefit the overall performance.

**ELECTRONICS AND COMPUTING**

The use of the **PC/104** stack meant that development time was minimal, as pre-built programs and code could be implemented and tested quickly on the platform without having to go re-compilation or porting. Nevertheless, **replacement of the PC/104** with a capable modern microprocessor would reduce the space, weight and power requirements of the **Computing Module** whilst maintaining equivalent capabilities.

**NAVIGATION**

Use of the networked **GPS system** showed the feasibility of using a Wireless LAN to disseminate positioning information amongst nodes or clients, though use of the system in a restricted or "urban-canyon" environment should be avoided as severe signal degradation occurs. An **alternative Urban-Canyon Navigational Aid** such as the new Antaris 4 SuperSense® Indoor GPS [42] would allow the vehicle to report accurate positioning information, whilst not requiring any modification to the existing LAN architecture.

**DATA STREAMING**

Use of an on-board QuickCam web camera showed that the idea of visual inspection was possible (which was expected), but it also showed that a redesign would be required if industry-standard pictures are to be obtained. A **software upgrade** and a switch to the **Real-Time Streaming Protocol** would allow the FireWire bus to be fully utilised providing video-streaming capabilities in addition to high quality still images.

## ACKNOWLEDGEMENTS

Firstly, I am deeply indebted to my supervisor Mr. Stephen Marais who endured two long years of equipment abuse and imprudent engineering decisions whilst never losing his composure.

Equal gratitude is due to Professor Andy Sass, I hope in the end I have managed to absorb a minutiae of the volumes you have tried to teach me.

Thanks to Glen Newins and the workshop staff, all of your hard work and accommodating attitudes were greatly appreciated.

Lastly thank you to my long-suffering parents for your unwavering support, I promise I will stop studying soon!

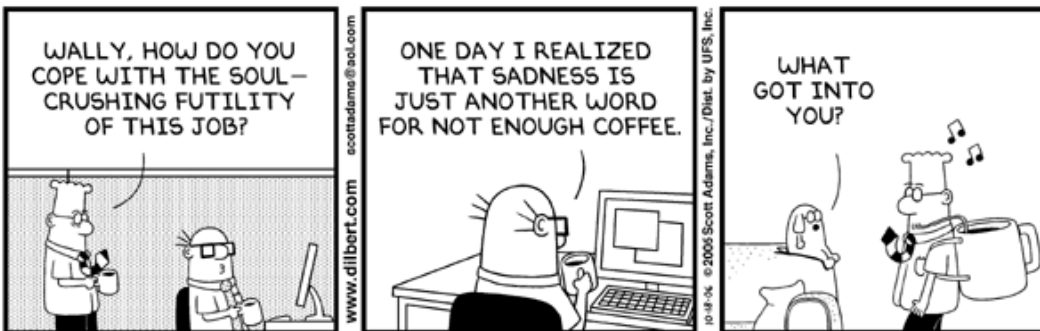
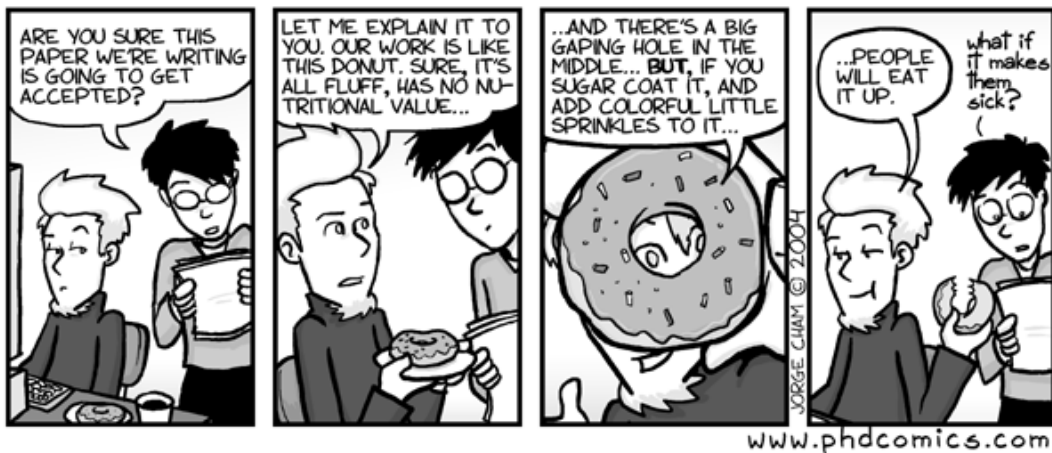


# TABLE OF CONTENTS

<b>SUMMARY .....</b>	<b>I</b>
<b>ACKNOWLEDGEMENTS.....</b>	<b>VI</b>
<b>TABLE OF CONTENTS .....</b>	<b>VII</b>
<b>LIST OF FIGURES.....</b>	<b>IX</b>
<b>LIST OF TABLES.....</b>	<b>XIII</b>
<b>1. INTRODUCTION.....</b>	<b>1</b>
<b>2. EROBOT: FINAL SOLUTION.....</b>	<b>10</b>
PERFORMANCE SPECIFICATIONS .....	12
2.1 SPECIFICATIONS: KEY .....	12
2.2 SPECIFICATIONS: TABLE .....	12
2.3 SPECIFICATIONS JUSTIFICATION .....	14
<b>3. DESIGN .....</b>	<b>15</b>
3.1 CONCEPTUAL DESIGN .....	15
3.2 MECHANICAL DESIGN .....	19
3.3 ELECTRICAL DESIGN .....	38
<b>4. COMMUNICATION, NAVIGATION &amp; CONTROL.....</b>	<b>46</b>
4.1 EMBEDDED COMPUTING.....	46
4.2 WIRELESS COMMUNICATIONS.....	53
4.3 GLOBAL POSITIONING SYSTEM (GPS) LOCATING .....	56
4.4 DATA STREAMING .....	60
<b>5. TESTING.....</b>	<b>61</b>
5.1 MOBILITY .....	61
5.2 CONTROL .....	62
5.3 NAVIGATION .....	62
5.4 DATA ACQUISITION .....	62

5.5	DUTY CYCLE.....	62
<b>6.</b>	<b>CONCLUSIONS &amp; RECOMMENDATIONS.....</b>	<b>63</b>
	<b>REFERENCES.....</b>	<b>66</b>
	<b>GLOSSARY &amp; ACRONYMS .....</b>	<b>70</b>
	<b>BIBLIOGRAPHY .....</b>	<b>72</b>
	<b>APPENDIX A: LITERATURE REVIEW .....</b>	<b>A1</b>
	<b>APPENDIX B: DESIGN AND MANUFACTURE.....</b>	<b>B1</b>
	<b>APPENDIX C: COMPUTER SYSTEM SETUP &amp; CODE.....</b>	<b>C1</b>

# LIST OF FIGURES

Figure 1-1: X-RAY Inspection of Electronic Components and <b>PCB</b> 's.....	1
Figure 1-2: The massive <i>Knock Nevis</i> .....	2
Figure 1-3: <i>Prestige</i> sinking .....	2
Figure 1-4: Robot Inspection Stations .....	3
Figure 1-5: Refinery 'bots.....	5
Figure 1-6: 'Bots for <b>HAZ</b> ardous <b>OP</b> erations <b>S</b> ( <b>HAZOPS</b> ).....	5
Figure 1-7: Wall climbers .....	6
Figure 1-8: Everest VIT: Rovver <sup>®</sup> Family .....	6
Figure 1-9: Marat <sup>®</sup> Inspection Robots .....	7
Figure 1-10: P3-AT.....	7
Figure 1-11: 2004 Thesis NDEbot .....	8
Figure 1-12: <i>Pinky</i> : A physical breakdown .....	8
Figure 2-1: eRobot attached to a vertical metallic plate .....	10
Figure 2-2: Overall dimensions.....	11
Figure 3-1: Trike concept .....	15
Figure 3-2: Trike: schematic.....	16
Figure 3-3: Reverse-Trike.....	16
Figure 3-4: Reverse-Trike schematic.....	17
Figure 3-5: Quad concept.....	17
Figure 3-6: Quad schematic.....	18
Figure 3-7: Exploded view .....	19
Figure 3-8: Drive Units .....	20

Figure 3-9: Gearbox components (left) and gearbox (right).....	21
Figure 3-10: Gearbox exploded .....	22
Figure 3-11: Gearbox showing shaft encoder and temperature sensor .....	22
Figure 3-12: Trial wheels.....	23
Figure 3-13: Re-designed wheel assembly .....	24
Figure 3-14: Machining the molds (left), the mold assembly (centre) and the vacuum setup (right) .....	24
Figure 3-15: Final wheel assembly .....	25
Figure 3-16: Frame .....	25
Figure 3-17: Testing chassis .....	26
Figure 3-18: Exploded view of frame.....	26
Figure 3-19: Frame weight reduction (left) and battery inserts (right).....	27
Figure 3-20: Frame: Partially assembled (left) and fully assembled (right) .....	27
Figure 3-21: Tail Unit.....	28
Figure 3-22: Rear (left) and exploded (right) .....	28
Figure 3-23: Finite Element Analysis .....	29
Figure 3-24: Hitch: Exploded .....	30
Figure 3-25: Machining of tail unit components .....	30
Figure 3-26: Tail Unit assembly .....	31
Figure 3-27: Payload Bay .....	31
Figure 3-28: Front showing FireWire camera .....	32
Figure 3-29: Front (left) and exploded view (right) .....	32
Figure 3-30: Front: Machining.....	33
Figure 3-31: Part, work-piece, manufacturing model .....	33



Figure 3-32: Tool-path generation & check .....	34
Figure 3-33: G-code simulation .....	35
Figure 3-34: Basic manufacture .....	35
Figure 3-35: Different materials & techniques.....	36
Figure 3-36: Multi-process machining.....	36
Figure 3-37: Extended one-piece machining.....	37
Figure 3-38: Initial prototypes (left) and final components (right) .....	37
Figure 3-39: <b>Electronics Module (EM)</b> .....	38
Figure 3-40: Bottom board (left) and H-Bridge recesses (right).....	39
Figure 3-41: Electronics: H-Bridge insets (left) and uBlox GPS (right) .....	39
Figure 3-42: Initial board .....	40
Figure 3-43: Thermal plot.....	40
Figure 3-44: Centre board (left) and GPS interface (right).....	41
Figure 3-45: Centre board .....	41
Figure 3-46: Part->.dxf->.brd->.tif ->assembly .....	42
Figure 3-47: DGPS board .....	43
Figure 3-48: Tool support and adaptor .....	44
Figure 3-49: Board manufacture: Testing .....	44
Figure 3-50: Board manufacture: Production.....	44
Figure 3-51: Assembled bottom board.....	45
Figure 3-52: Board assembled (left) and installed in robot (right).....	45
Figure 4-1: The PC/104 "stack" (rendered) .....	46
Figure 4-2: Advantech PCM3370 .....	47

Figure 4-3: RTD DM6420.....	48
Figure 4-4: RTD DM6816.....	48
Figure 4-5: Advantech PCMCIA Expansion Card .....	49
Figure 4-6: FireWire®/USB 2.0 Expansion Board .....	49
Figure 4-7: SOFTWARE: gpsd, GpsDrive and Apache .....	51
Figure 4-8: Website running on eRobot .....	52
Figure 4-9: Screenshot: Xawtv.....	52
Figure 4-10: LAN.....	53
Figure 4-11: Full LAN architecture .....	54
Figure 4-12: TCP vs UDP .....	55
Figure 4-13: Overall control.....	56
Figure 4-14: Antaris RCB-LJ receiver.....	57
Figure 4-15: DGPS setup.....	59
Figure 4-16: UniBrain Firewire camera (left) and QuickCam Pro (right) .....	60
Figure 5-1: Testing of vehicle on a vertical ferro-magnetic board .....	61
Figure 6-1: Antaris SuperSense® data in a shopping mall.....	64

---

## **LIST OF TABLES**

---

Table 1 : Specification Table Key .....	12
Table 2: uBlox Antaris features .....	57
Table 3: NMEA data structure .....	57
Table 4: uBlox data structure.....	58



An Industrial NDE robot

**[This page is intentionally left blank]**

# 1. INTRODUCTION

## BACKGROUND

This report details the design and development of an industrial inspection robot capable of carrying **Non-Destructive Evaluation (NDE)** equipment and performing NDE tests.

Since the early 1950's, NDE has been revolutionizing all fields of industry but particularly production and maintenance. For the manufacturing sector, the widespread implementation of accurate NDE techniques (such as ultrasonic inspection) as well as the introduction of fracture mechanics, allowed engineers to more accurately predict the lifetime of components before failure [1], leading to an increased rejection in faulty or sub-standard components.

A similar revolution took place in sectors involved with maintenance and inspection. Flaw detection and *characterisation* (the classification of the *type* of defect) would enable technicians to establish whether failure was imminent or if there was still a substantial safety margin, thus striking a balance between safe operation and costly maintenance downtime [2].

NDE has facilitated accurate, rapid inspection ranging from the smallest of components to entire structures. Shown in **Figure 1-1** below are images of various electronic components and **Printed Circuit Boards (PCB)**. Visible on the left frame is an X-Ray scan of a modern die for an **Integrated Circuit (IC)** chip. The centre image shows a through-hole in a multi-layer PCB that has not been fully plated due to poor solder re-flow and the right frame highlights inconsistencies in drill spacing on another PCB [3].

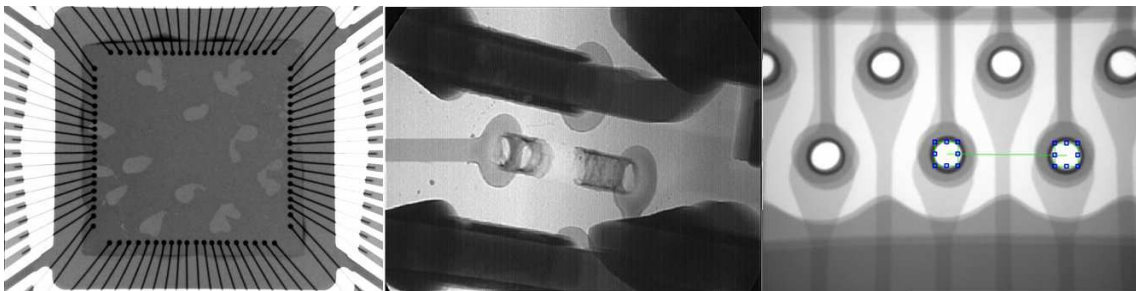


FIGURE 1-1: X-RAY INSPECTION OF ELECTRONIC COMPONENTS AND **PCB'S**

NDE is not confined to the small and **Figure 1-2** overleaf shows one of the largest ships in the world, the *Knock Nevis*. The *Knock Nevis* is a *supertanker*, or a transport vessel that is capable of transporting more than 500,000 deadweight tonnes of crude oil [4].

FIGURE 1-2: THE MASSIVE *KNOCK NEVIS*

This particular vessel is in excess of 480 metres in length and has a 69 metre girth, and detailed inspection of her internal compartments is a huge, but vital, task.

Even in an enormous freighter such as the *Knock Nevis* small internal flaws in the hull could lead to failure of the structure as a whole, with disastrous consequences. Structural integrity has led to many maritime disasters, one of which is shown in **Figure 1-3** below:

FIGURE 1-3: *PRESTIGE* SINKING

This unfortunate photograph is of the Japanese-built, Greek-operated, Bahamas-registered and Liberian-owned *Prestige* sinking off of the Spanish *Costa de la Muerte* (Death Coast) in late 2002[5]. The *Prestige* was bound for Singapore and carrying 77 000 tonnes of crude oil, and the resulting slick had enormous environmental, social and economic impacts on the region. Fishing restrictions were enforced along the coastline, depriving communities that depended on the sea of their livelihood.

Criticism was heaped upon the shipping community, one claim being that single-walled vessels were no longer suitable for the transport of damaging content such as crude oil [6] (*Exxon Valdez*, which ran aground in Prince William Sound, Alaska, causing massive environmental damage, was also of single-hull construction [7]). Another single-hulled vessel the *Erika* sank off the coast of France in 1999, and the subsequent *Prestige* sinking prompted the **European Union (EU)** to call for a phasing-out of single-hulls to be completed by 2015 [6].

Severe structural degradation was cited as being one of the primary factors for the ship's hull splitting clean in half [8]. After the accident, the EU called for an increase in the

number of inspections conducted on dangerous freights from once to twice yearly, putting under pressure maintenance workers who were already struggling with the initial inspection quota [6].

Analyzing the entire structure of such a vessel for structural deficiencies is an incredibly manpower-intensive task, requiring the vessel to spend extended periods of time in dry-dock. According to Mr. Jonathan Wamsteker - owner and operator of Sonometrics, a Cape Town based marine inspection company - a medium sized cargo vessel could spend four to five months in dry-dock if it had to undergo detailed inspection.

Traditional methods employed in industry call for rope-access inspection teams to conduct NDE inspection on the sides of the vessel by hand [9]. This is a lengthy process and in addition the working conditions in the dock are hazardous to NDE personnel.

The implementation of a robotic inspection solution would not only eliminate the danger to on-site NDE personnel but could also afford other advantages such as reduced inspection time.

### **Robotics & NDE**

Robotics as an industry has experienced rapid growth fuelled by the massive boom in the electronics and computer industries [10]. These advances have allowed the replacement of human technicians with robot stations, as is becoming increasingly commonplace in industry. **Figure 1-4** shows a weld inspector checking mounts on a nuclear reactor vessel [11]. Adjacent to the weld inspector is *BONNIE III*, a non contact ultrasound nuclear boiler inspector. [12]



FIGURE 1-4: ROBOT INSPECTION STATIONS

Applications of robotics in a fairly standardised, repetitive environment such as an assembly line or inspection station is markedly different to the implementation of an inspection system in a marine dry-dock. Environmental conditions inside a modern factory are tightly controlled, whereas a robot operating in a marine environment will have to deal with all types of real-world phenomena, ranging from hostile weather conditions to careless dockside personnel.

However, implementation of such a system would afford NDE personnel safer working conditions as well as potentially reducing inspection time. This combination of factors illustrated the need for the implementation of robotics and automation.

Mr. Wamsteker was first struck with the idea and approached the Department of Mechanical Engineering at UCT to propose the idea as a research project. Consultation with Mr. Wamsteker yielded the basis of the design requirements (a full set of which can be found in the Performance Specifications section beginning on page **12**).

The first criterion was centred on the vehicle's ability to traverse a ship's hull. Mr. Wamsteker indicated that a vehicle that could attain a straight-line speed of 0.5 m/s would provide suitable capabilities for rapid inspection.

Operating in the testing environment of the dry-dock, the platform is required to be reliable with a low maintenance overhead. Effectively, this meant that the robot should only need to be recharged at the end of the day (meaning a 6-8 hour operating cycle) and should not require maintenance more than once a week. The duty cycle was determined to be too demanding for the project initially, and was revised down to two hours.

Mr. Wamsteker also stressed the need for the vehicle to be remotely controlled. He noted that some ships were in excess of 6 stories high from the bottom of the dry-dock, and as such the operator should still be able to control the vehicle. As such, 30 metres was agreed to be the minimum range for the robot.

A simple, user-friendly interface would allow marine technicians with a minimum of training to operate the vehicle. Lastly, the project is required to be commercially competitive with currently available inspections, including manual inspection.

### **CURRENT TECHNOLOGICAL TRENDS**

As a result of the growth of robotics as an industry, increasingly more systems are being developed that are capable of conducting NDE inspection. The petroleum sector is an avid proponent of remote NDE technology, due to the huge amount of piping networking and storage vessels that comprise a petroleum refinery, where even a mid-size oil refinery may have in excess of 350 miles of piping [13].

Need for pipeline inspection was highlighted by the February 2006 spill at Prudhoe Bay in Alaska, site of the **Beyond Petroleum (BP)** Prudhoe Bay Oil Field where 16 "anomalies" (highly corroded regions) were thought to be in one section of pipe. However on detailed inspection after the spill it was found there were over five thousand [14]. Spills such as these have major ramifications in terms of environmental cleanup costs [15].



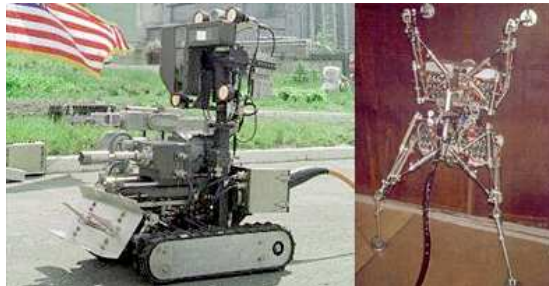


FIGURE 1-5: REFINERY 'BOTS

**Figure 1-5** shows two robots development for use in petroleum and petrochemical environments. *Neptune*, on the left, is a petroleum-storage inspection vehicle [16]. It can navigate on either the internal or external side of the tank, and adheres to the tank by means of magnetic drive tracks. The sensor payload consists of a video camera and **Ultrasonic Testing (UT)** equipment to conduct detailed inspection. Power is provided to the unit by means of a tether which also provides a data bus to and from the vehicle.

**Figure 1-5's** right panel is an image of the *Explorer II*, a dedicated gas pipeline inspection robot funded by the United States **Department of Energy (DoE)** [17]. The *Explorer* is a wireless NDE inspection unit capable of evaluating the structural integrity of pipelines. The system makes use of a modularised design to house its on board electronics and cameras. Design in this fashion not only exploits the advantages of modularity, but it also allows the vehicle to turn through bends in pipes, as well as ascend vertically.

Robots are aptly suited to other hazardous applications, one popular example being pressure vessel inspection in nuclear reactors.

FIGURE 1-6: 'BOTS FOR **HAZARDOUS OPERATIONS (HAZOPS)**

Shown in **Figure 1-6** are two inspection robots. On the left is *Pioneer*, a vehicle designed and developed at one of the powerhouses of modern robot development, the Robotics's Institute at Carnegie Mellon University [18]. The primary mission for *Pioneer* was the inspection of Reactor 4 at Chernobyl power station in the Ukraine. Pioneer carries an impressive array of environmental sensors in addition to an onboard core-borer (for retrieving material samples on-site) as well as a mapping unit for creating 3D models of the interior structure of the reactor.

In the adjacent photo is the *ROBUG II*, designed at the Department of Electronics and Computer Science at the University of Southampton in the United Kingdom. *ROBUG II* is a legged robot capable of performing autonomous floor to wall transfers, and is ideally suited for conducting inspection in environments with very limited access (such as nuclear reactor pressure vessels) [19].

Inspection of a ship-hull will require a robot platform that can easily traverse the hull, all the while remaining firmly adhered. A cross-section of some of the alternative Research and Development (R&D) dedicated wall-climbing robots are shown in **Figure 1-7** below:

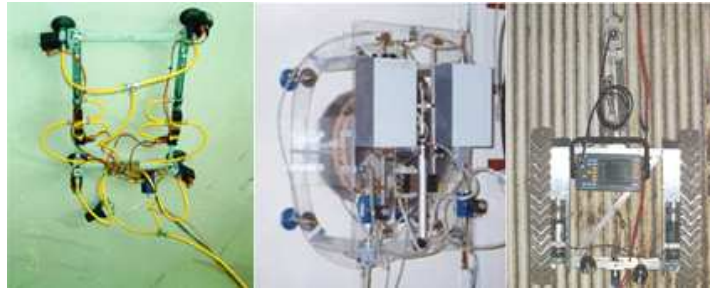


FIGURE 1-7: WALL CLIMBERS

On the left in **Figure 1-7** is *WALLY*, developed by the *Dipartimento Elettrico Elettronico é Sistemistico (DEES)* of Catania University [20]. *WALLY* is a prototype robot designed to conduct surface inspection on industrial chimneys and storage tanks. The centre panel shows an image of *SURFY*, also developed by DEES, which is another articulated pneumatic-powered inspection robot [21]. The **Tennessee Technical University Centre for Energy Systems Research (TTU CESR)** robot on the right was developed to analyse the thickness of water-walls in coal fired power plants [22].

In industry, commercial inspection robots are readily available for a variety of tasks.



FIGURE 1-8: EVEREST VIT: ROVVER® FAMILY

Shown in **Figure 1-8** above are the Rovver® family of visual inspection robots from Everest VIT (now amalgamated into General Electric® Inspection Technologies), mainly for remote pipeline inspection [23]. The smallest member of the family is (the R400, leftmost 'bot in **Figure 1-8**) capable of conducting inspection in pipe diameters as small as 4" (~100mm). Maximum range for the series is 200 metres and the largest version,

the R900 (**Figure 1-8**, right) is capable of carrying additional sensory equipment for other inspection tasks.



FIGURE 1-9: MARAT<sup>®</sup> INSPECTION ROBOTS

Similar to the Rovver family are the MARAT<sup>®</sup> series of industrial inspection/cleaning robots. The MARAT robots use a common chassis and different payload modules to fulfil different tasks [24].

One of the major disadvantages of commercially available platforms is cost. For example, the P3-AT, a commercial robot platform targeted at developers (shown in **Figure 1-10**) costs in excess of US\$3 000, just for the base unit. Some of the more advanced systems cost upwards of USD\$70 000 [25].



FIGURE 1-10: P3-AT

As such one of the design criteria that the project will aim to fulfil will be the development of an equivalent system that would be able to compete commercially in the market-place.

From this brief [and by no means exhaustive] overview, it becomes apparent that there are multitudes of inspection systems available and in development, involving both standard inspection NDE techniques as well as more advanced ones such as ultrasound.

Each system has unique attributes that facilitate its function; however, no system completely fulfils the exact requirements of Mr. Wamsteker and as such a new system would have to be developed.

#### **PREVIOUS DEVELOPMENT**

Development of a dedicated NDE capable robot was the subject of a 2004 conjoint undergraduate thesis project [26] [27]. Shown in **Figure 1-11** overleaf is the end result of the project, dubbed *Pinky*.



FIGURE 1-11: 2004 THESIS NDEBOT

*Pinky* utilised standard Phillips<sup>®</sup> electric screwdriver motors as drive units. Visible in the left frame of **Figure 1-12** is the aluminium frame and the drive units arranged in pairs, located at the front and rear. Adhesion was accomplished with custom-sintered cylindrical rare-earth Neodymium magnets, one of which was located on each of the four drive wheels.

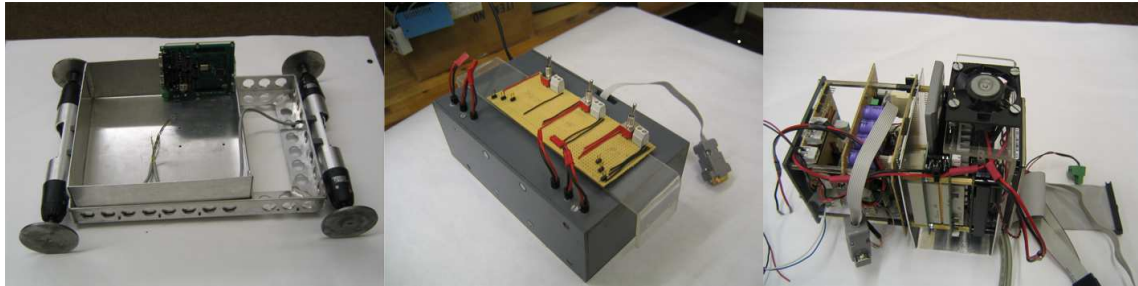


FIGURE 1-12: *PINKY*: A PHYSICAL BREAKDOWN

Inspection was performed with a modified Panametrics<sup>™</sup> hand-held ultrasonic thickness gauge (encased in a protective housing, visible in the centre panel of **Figure 1-12**) with control being implemented with an embedded PC/104 computer and custom circuitry (**Figure 1-12**, right panel).

As a primitive test-bed, the NDEbot performed adequately. However, while the vehicle was capable of adhering firmly to ferro-magnetic walls, it was not capable of turning or ascending vertically. The modified (some would say jerry-rigged) NDE payload was also subject to regular inconsistencies.

In order to produce a platform that would be capable of performing in an industrial environment, major improvements had to be made to the concept. These included (amongst others): ruggedization of the platform, expansion of the NDE techniques used as well as cost evaluation of the platform, as a whole, to ensure market competitiveness.



An Industrial NDE robot

This project took the experiences gained from the first NDE prototype and incorporated them into the next generation NDEbot. The report begins with a description of the platform, followed by an examination of all the major aspects contributing to its performance. Concluding the report is a discussion with respect to recommendations for future work.



## 2. **ERObOT: FINAL SOLUTION**

[For video footage of the robot in action, please see the accompanying DVD.]



FIGURE 2-1: EROBOT ATTACHED TO A VERTICAL METALLIC PLATE

**eRobot** is a 2<sup>nd</sup> generation inspection robot. It fuses the power of modern embedded computing technology with the diversity of low-cost robotics. Primarily designed for the inspection of marine vessels in dry-dock, eRobot makes use of a highly modular design in order to be able to fulfil a variety of inspection tasks.

Custom-sintered magnets and custom made drive-units allow eRobot to adhere to ferro-magnetic structures and to travel inverted if required.

Communication is realised over a standard wireless (**WiFi**) network and utilises a standard LAN architecture to provide full internet connectivity, allowing the logging of position and data to its associated server and website.

Control of the robot is made possible by a standard joystick and laptop, giving the operator full and intuitive control of the vehicle. An embedded computer running open-

source software and utilising custom communication and control programs ensures a rapid and accurate response to any user-input.

Making use of Differential GPS technology, eRobot is capable of downloading correctional data from its associated DGPS server, allowing for accurate 3-dimensional positioning.

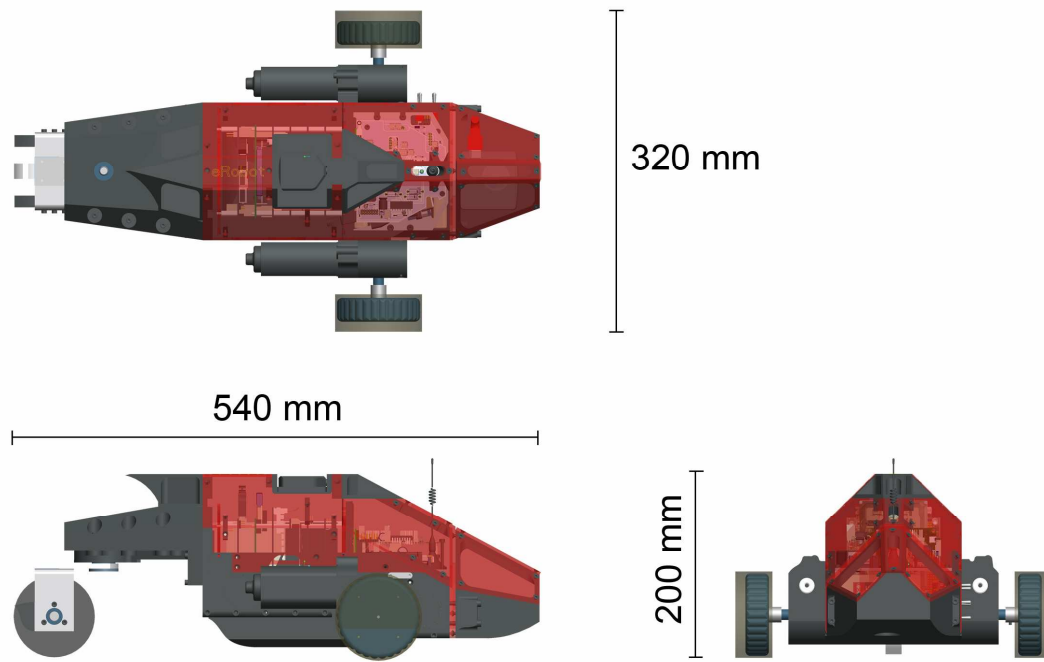


FIGURE 2-2: OVERALL DIMENSIONS

## Performance Specifications

### 2.1 Specifications: KEY











Specification Table Key	
Critical	
Advantageous	
Desirable	
Achieved	
Fully implemented	
Partial implementation	
Not Implemented	

TABLE 1 : SPECIFICATION TABLE KEY













Shown in **Table 1** above is the Specification Table key. The top section describes how each performance criteria was rated. A **critical** aspect of the design was part of the original design specifications as were discussed with Mr. Wamsteker.









An **advantageous** criterion was one which was mentioned by Mr. Wamsteker as being potentially useful, however it was not paramount to the success of the project. Lastly, a **desirable** attribute was one added by the author as an aspect that could be potentially useful to the end-user. The *Achieved* section details the degree of implementation of the design criteria. **Three bars** show a full implementation of the criterion, **two bars** infers a partial or incomplete implementation with more development required. **One bar** means there was no attempt at implementation.





### 2.2 Specifications: TABLE

SPECIFICATION	DESCRIPTION	RATING	ACHIEVED
Physical Attributes			
Minimum straight line speed	0.5 m/s		
Manoeuvrability	Full manoeuvrability with sufficient adherence to travel inverted.		



Operating Range	Minimum operating Range of 30 metres		
Operating Cycle	Operate continuously for a period of at least 2 hours		
Multiple Payloads	Accommodate a variety of NDE techniques		
Modular Design	Allow for incorporation of alternate NDE payloads or drive techniques		
Weight	To weigh no more than 8kg's, to facilitate easy transport by one operator		
Profile	Have a cross-sectional area small enough to allow travel in standard 14" piping		

Control & Interface			
Human Interface	Easy video-game like intuitive user control, minimal learning or training		
Expandability	Allow for implementation of self navigation and environmental awareness		
Data Acquisition	3D mapping enabled to present data in a simple effective way		
Media Feed	Real time streaming to allow user a robot view perspective		

SPECIFICATION	DESCRIPTION	RATING	ACHIEVED
<b>Miscellaneous</b>			
Commercially competitive	Economically must compete with equivalent market-available platforms & techniques		
Expansion & Upgradeability	Allow for incorporation of more efficient/advanced techniques.		

## 2.3 Specifications Justification

From the specifications table it can be seen that not all major requirements were fully met. In particular, these were the straight-line operating speed and the duty cycle.

### STRAIGHT LINE SPEED

A minimum of 0.5m/s was specified by Mr. Wamsteker in the initial design specifications. When the robot was tested, it was found that the bot could only attain 0.2 m/s. As such, it failed the initial criteria; however suggestions for design modifications have been made in the **Recommendations** section in order to improve the vehicle's speed.

### DUTY CYCLE

A duty cycle of 2 hours was initially outlined for the platform, having been throttled down from the initial 6-8 hour specification. This full extent was unfortunately never tested due to the failure of some equipment in the testing process.

This is fully documented in the **Testing** section, and recommendations for performance improvement have been made in the **Conclusions & Recommendations** section on page **63**.

## 3. DESIGN

As is the case with any cross-disciplinary project, the design of eRobot spanned a number of engineering fields. Before any detailed or embodiment design work was undertaken, a conceptual design phase was performed, forming the basis of the upcoming detailed design phase.

From the conceptual design, detailed mechanical and electrical design phases were performed, providing the necessary schematics and data for manufacture.

### 3.1 Conceptual Design

Various conceptual robot configurations were envisioned for the new generation robot, bearing in mind the successes and failures of the preceding prototype. This generation of robot had to address the previous inadequacies that were highlighted by the initial design.

Specifically, this involved the drive configuration, as this was where the initial prototype underperformed substantially.

#### TRIKE

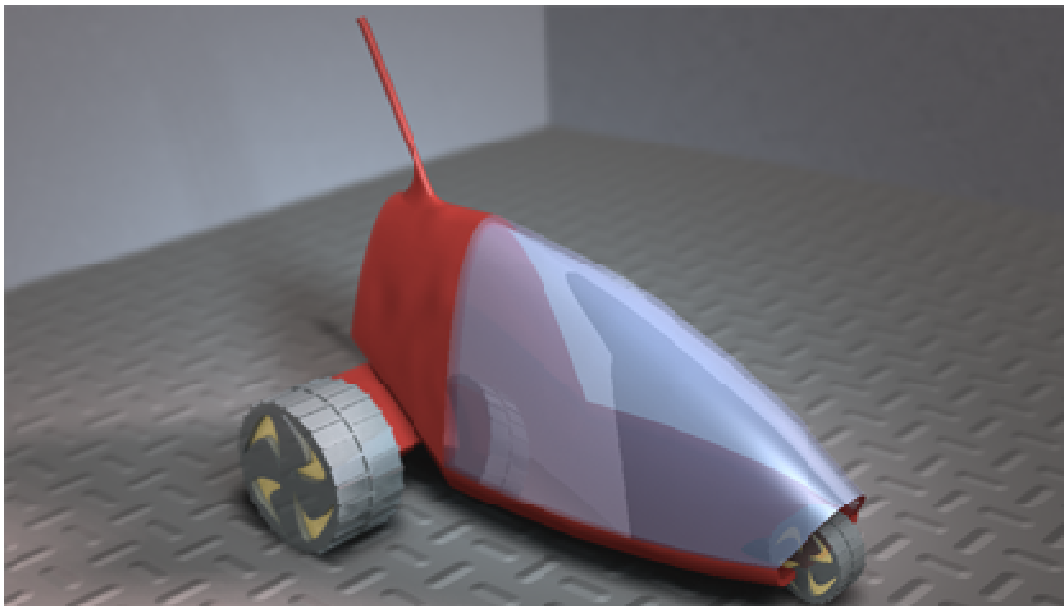


FIGURE 3-1: TRIKE CONCEPT

Conceptually, the trike concept has a number of advantages over a conventional 4-wheeled design. All drive elements are located at the rear, and steering could be accomplished merely by either varying speed of each drive wheel with a front neutral “jockey”, or by having an active steering nose wheel and standard rear wheel drives.

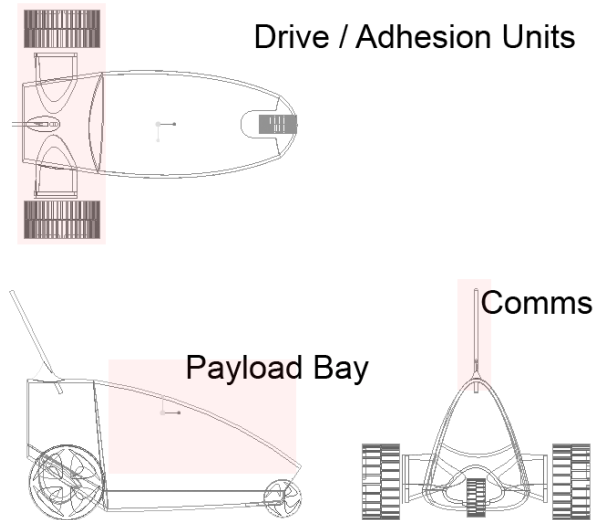


FIGURE 3-2: TRIKE: SCHEMATIC

Although simplistic in nature, this version of the **trike** concept did not lend itself to the envisioned modular design as much as other concepts, and was discarded.

#### REVERSE TRIKE

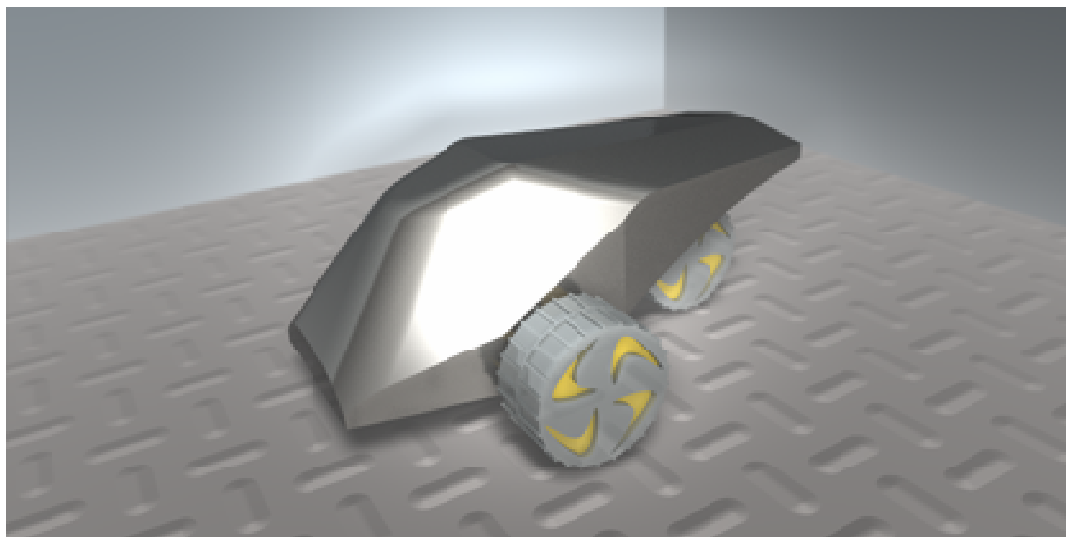


FIGURE 3-3: REVERSE-TRIKE

This concept is similar to the **trike** concept outlined above, but differentiated by having the drive wheels near the front of the vehicle, and the trailing neutral “jockey” at the rear. Having the drive/adhesion units in this configuration would allow the substitution of drive units and/or payload without the need for major reconfiguration.

## EROBOT

An Industrial NDE robot

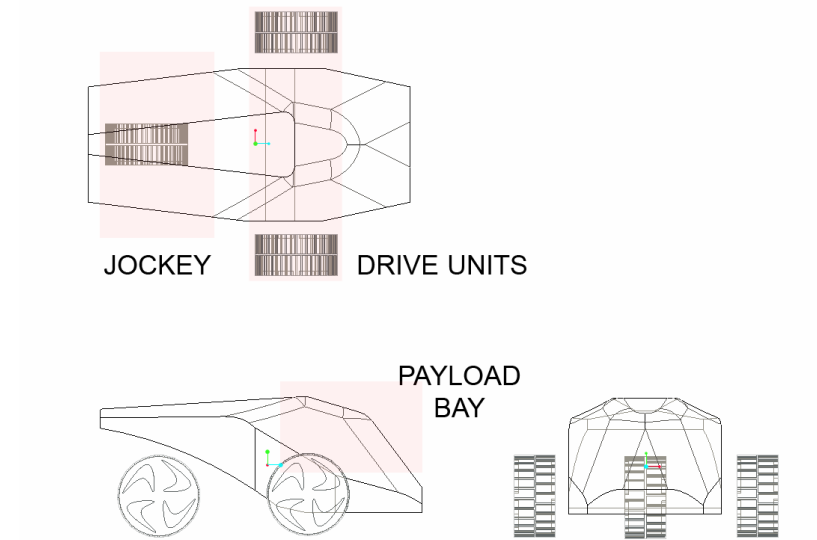


FIGURE 3-4: REVERSE-TRIKE SCHEMATIC

### QUAD

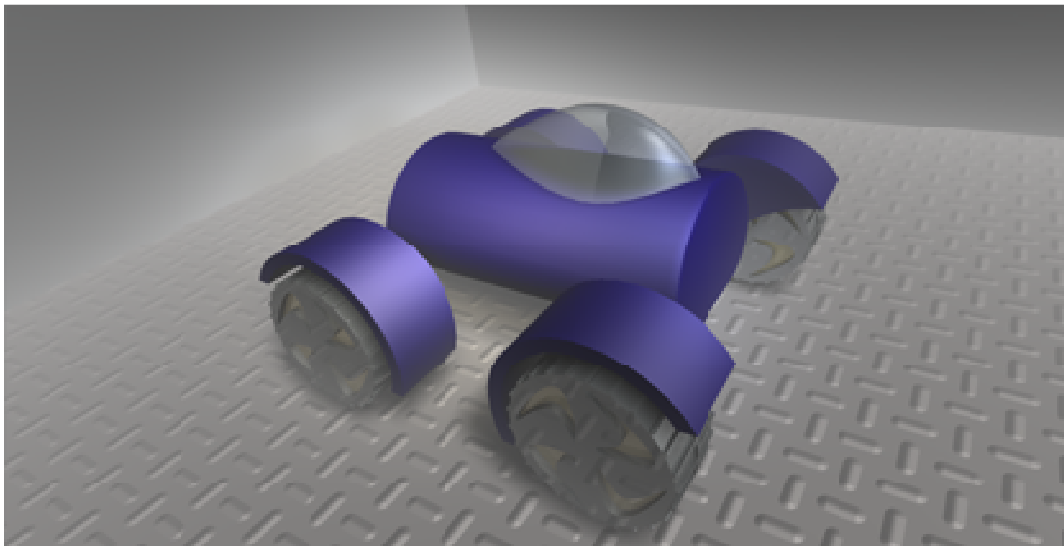


FIGURE 3-5: QUAD CONCEPT

This concept, due to its inherent simplicity was the one selected for the first generation of robot. In addition, with four wheels instead of three, the **quad** provides more adhesive power than the previous two concepts.

However, due to the demanding requirements of adherence and low rolling friction, the quad concept requires substantially more driving control than the other two concepts. This was due to the fact that the wheels, due to the intense adhesive force of the magnets, did not allow for any "scuffing". Therefore if this concept was

to become viable, a differential drive system would have to be developed, adding substantially to the complexity of the design.

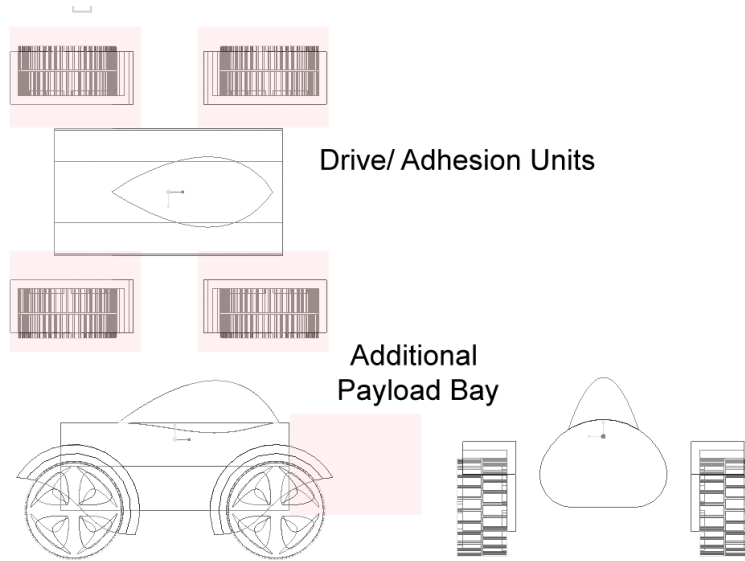
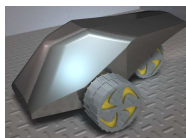


FIGURE 3-6: QUAD SCHEMATIC

Although the **quad** concept was more accommodating for a modular design, the difficulties in implementing a successful driving system eliminated it as a viable concept.

#### SELECTED CONCEPT



Previous experience with the **quad** concept had shown a number of deficiencies inherent in the design. A lack of perceived expandability eliminated the concept of the **trike**. As such, it was decided that the **reverse-trike** offered the most advantages, and was selected.

## 3.2 Mechanical Design

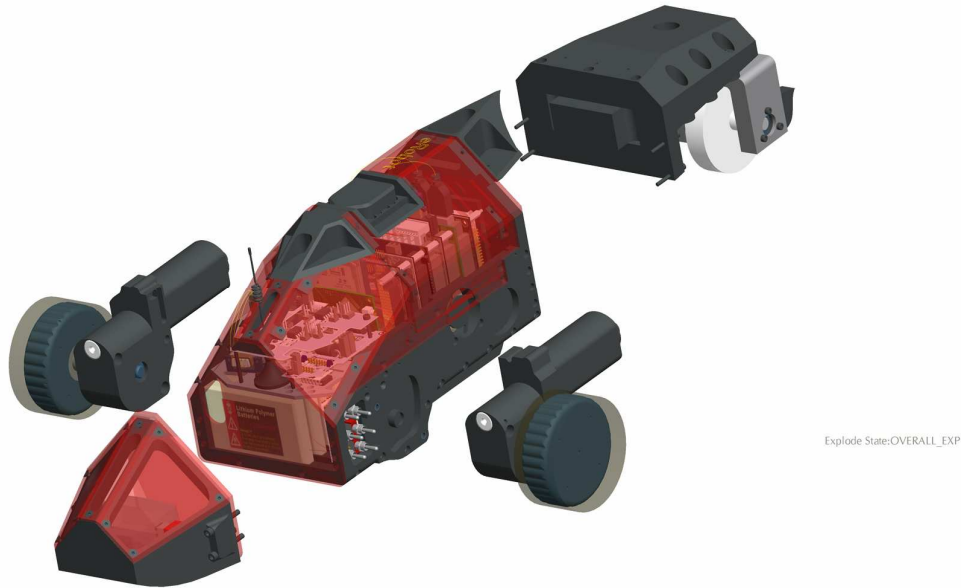


FIGURE 3-7: EXPLODED VIEW

Detailed design of the platform had to take into account several factors:

### **MODULARISATION**

Paramount to the success of the robot was its ability to adapt to different environments. Developing a drive system that was capable of adhering to (and providing grip on) ferro-magnetic surfaces **and** being capable of traversing other environments (such as the interior of a piping network) successfully would have been an exceedingly complex task.

Instead the entire design was conceived as a system of modules, which could be configured appropriately depending on the environment. For the case of marine inspection, three magnetic wheels were required, however if the 'bot was used in a standard "rover" role, they could be substituted for a set of large non-magnetic high-profile wheels.

Therefore each module had to be self-contained with only the minimal amount of connections required to other modules, as extensive need for assembly/disassembly would negate the entire purpose.

### **MATERIAL SELECTION**

From the outset, **High Density Poly-Ethylene (HDPE)** was chosen as the material of choice. HDPE is a low cost urethane plastic with a number of characteristics that make it useful for robotic construction. Primarily, HDPE is cost effective with most standard thicknesses below 40mm being readily available in a variety of colours. It

is also easy to machine, with high cutting speeds being used (up to and including 1000mm/min 5mm deep cuts) leaving an excellent surface finish.

Orange Perspex® was used primarily in the canopy construction, and gave the platform an aesthetic appeal. However, Perspex also is very tough and provided good structural reinforcement, particularly for the front section of the frame.

### **FABRICATION**

To reduce manufacturing errors to a minimum, all parts were designed to be machined on the Department's CNC Centre, consisting of a 3-Axis Milling machine and a 2-Axis Lathe.

However, the work envelope of the CNC mill was only 300mmx250mmx250mm (Length, Width and Height). Therefore each module (or the components that it consisted of, if it was not one-piece) had to fit comfortably inside the mill's work volume.

### **DESIGN CRITERIA**

As with any remote self-powered application, the lighter the platform the less demanding it is in terms of power requirements. Therefore, use of **Finite Element Analysis (FEA)** techniques to determine the optimal design in terms of structural integrity and weight were considered.

Previously regarded as a post-design add-on, the infusion of aesthetic appeal to the platform should proceed conjointly with the Mechanical and Electrical design, ensuring the 'bot was not only functional, but also pleasing to the eye.

Taking into account these design criteria, the following sections analyse the design of each module.

### **DRIVE UNITS**

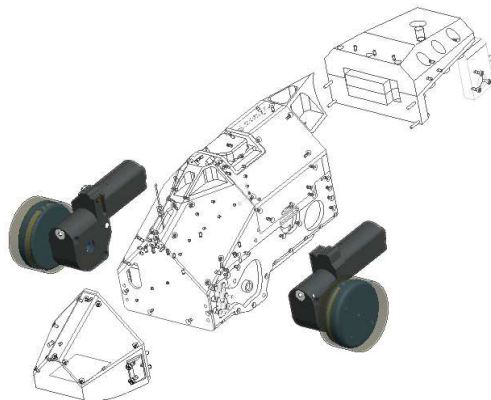


FIGURE 3-8: DRIVE UNITS

As eRobot was designed destined initially for marine inspection, its capacity to adhere to vertical surfaces was critical. As such, design and fabrication of the drive



units was one of the most critical aspects of the design. A number of design iterations had to be performed before a solution was reached.

In the initial (1st Generation) prototype, electric-screwdriver motors were used. These provided insufficient power to effectively move the platform vertically, and therefore other motors had to be sourced.

A relatively inexpensive alternative was to use standard windscreen-wiper motors, which are readily available from car-breakers and motor spares shops. They run off of 12V, and are specified to provide up to 1Nm of Torque [28]. However, they are notorious for power consumption (running under full load, it was seen that a single motor could consume up to 3 Amps at 12V!).

Preliminary housings were developed and tested to evaluate the motor's performance.



FIGURE 3-9: GEARBOX COMPONENTS (LEFT) AND GEARBOX (RIGHT)

Shown in **Figure 3-9** are the components of the first gearbox and the gearbox itself. This initial 'box' was a 3-piece assembly, and there were issues in locating the rotor completely accurately within the housing. Any amount of play led to either the rotor locking completely, or failing to mesh with the helical drive gear. However, with careful assembly (and the use of shims) two functional gearboxes were assembled and used in an initial test vehicle (see the **Frame** section), showing the concept to be feasible.

Once the validity of the design was proven, an improved version of the gearbox was designed. The new design reduced the number of structural components from three to two (allowing for more precise location of the rotor) in addition to incorporating weight saving features.

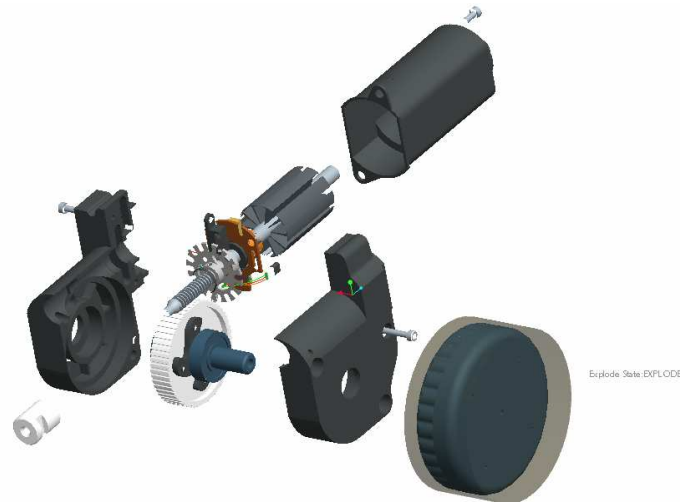


FIGURE 3-10: GEARBOX EXPLODED

**Figure 3-10** shows an exploded view of the final design. This design also incorporates a notched aluminium shaft encoder, as well as recesses for the accompanying opto-isolator. In addition, a temperature sensor was mounted on the interior of the motor casing to allow for monitoring of the thermal performance of the motor.

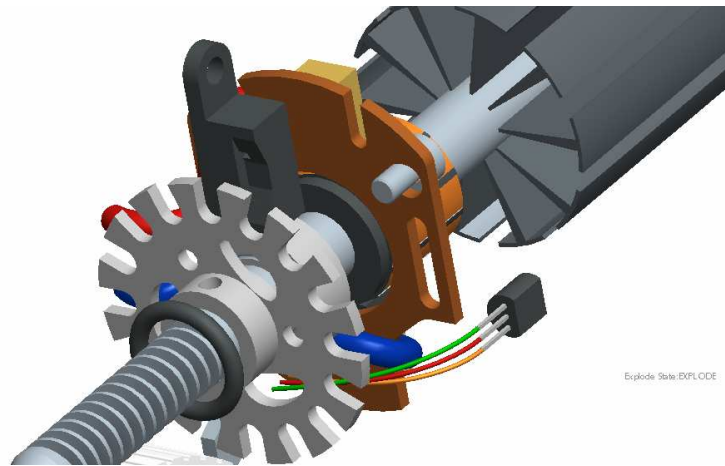


FIGURE 3-11: GEARBOX SHOWING SHAFT ENCODER AND TEMPERATURE SENSOR

In order to adhere to a vertical ferro-magnetic surface (such as a ship-hull) eRobot made use of permanent rare-earth Neodymium magnets. However, neodymium rare earth magnets are very brittle as a result of the sintering process and require some sort of protection. The magnets are also very smooth, and afford almost no traction. As such, a wheel assembly had to be designed that would accommodate the magnet and allow it to adhere to an underlying ferro-magnetic surface, while simultaneously protecting it from the harsh working conditions and providing grip on the surface.

Material selection for the wheels was not trivial, and a variety of compounds and techniques were evaluated before a solution was reached.



FIGURE 3-12: TRIAL WHEELS

Initially, plain electrical shrink-tubing was used around the wheel; however this exhibited very poor traction and wear characteristics. On consultation with **Advanced Material Technologies (AMT)** (a Cape Town based composite speciality company), it was decided that a casting-silicon “shoe” would be preferable to plain shrink-wrap.

In **Figure 3-12** (left), the (destroyed) silicon shoe can be seen in the lower-right corner. Although displaying better traction and wear characteristics than the shrink-tubing, it lasted a mere 10 minutes of testing.

An alternative composite, a casting poly-urethane was evaluated next (**Figure 3-12**, right), and this showed exceptional traction capabilities. However, resilience was again an issue and the shoe did not last substantially longer than the previous attempts.

It was noted that the casting procedure used left a substantial number of air bubbles in the mix, degrading the structural integrity of the compound. In addition, the ridged galvanised steel discs whose purpose was to provide a greater area for adhesion of the matrix only served to initiate tears on the inner surfaces of the shoe, rapidly leading to failures.

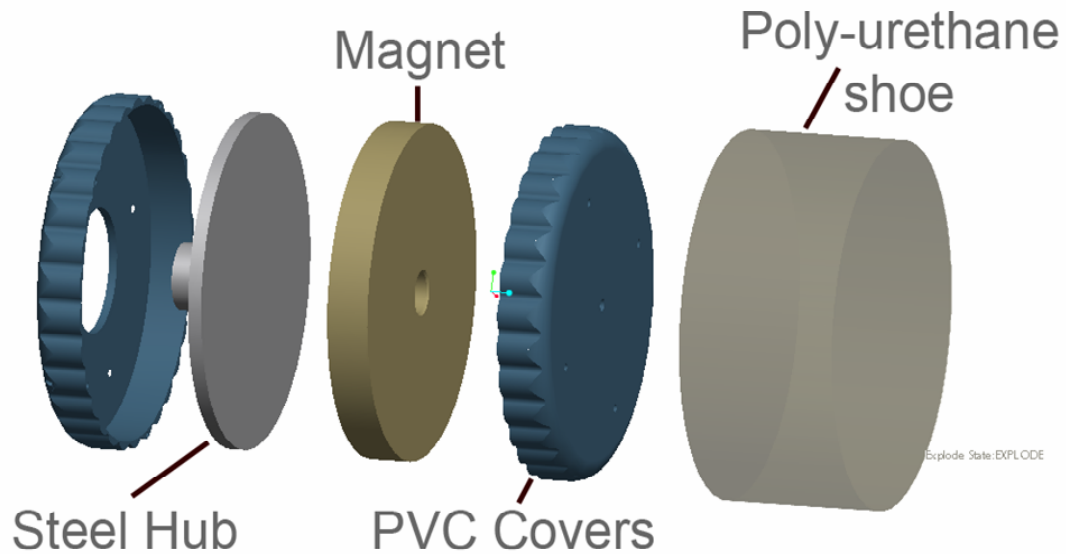


FIGURE 3-13: RE-DESIGNED WHEEL ASSEMBLY

The solution (as seen in **Figure 3-13**) was to redesign the wheel assembly with PVC covers eliminating the sharp inner edges. In addition casting of the entire wheel was performed in a vacuum chamber to reduce the number of air bubbles present.

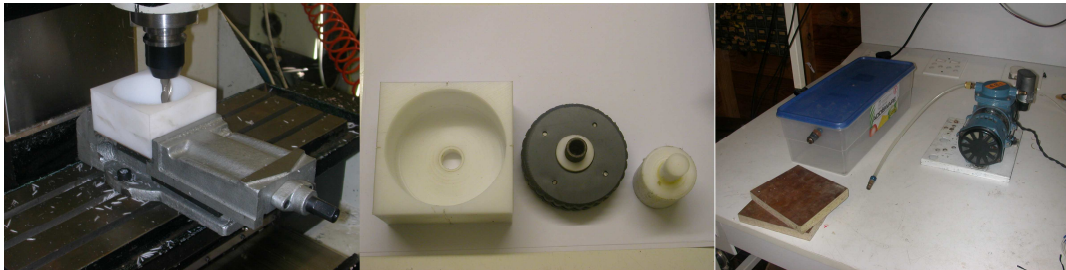


FIGURE 3-14: MACHINING THE MOLDS (LEFT), THE MOLD ASSEMBLY (CENTRE) AND THE VACUUM SETUP (RIGHT)

Shown in **Figure 3-14** are the steps for casting the wheel. First the mold negative was machined on a CNC milling machine (left), the wheel assembly to be cast was assembled (centre) and placed in a home-made vacuum-chamber (right) which consisted of a vacuum pump and a reinforced Tupperware<sup>®</sup> container. Setting time was specified on the packaging to be 16 hours, however due to the cold weather at the time (temperatures were in the 15-19°C range), each wheel took approximately 24 hours to set completely.



FIGURE 3-15: FINAL WHEEL ASSEMBLY

This final revision, with smoothed internal surfaces and reduced air-bubble content exhibited markedly better performance in terms of both traction and resistance to wear, and in fact lasted the entire length of the project without needing replacement.

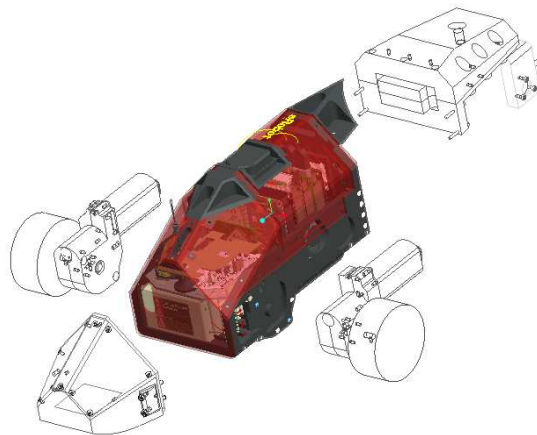
**FRAME**

FIGURE 3-16: FRAME

Core to the entire robot is the main chassis or **frame**. The premise behind the frame was that it would remain central to the system, capable of interfacing with a variety of drive units and sensor arrays.

In order to evaluate the viability of the frame, and its capacity to carry load, a trial unit was constructed. Shown in **Figure 3-17** overleaf is the preliminary chassis used to evaluate the performance not only of the chassis as a structural member, but also of the load carrying capabilities of the robot and the viability of using the rear wheel as a free-slipping jockey.





FIGURE 3-17: TESTING CHASSIS

In this test the robot chassis was powered from a standard bench power-supply, and its ability to manoeuvre in the vertical plane was evaluated. (For the videos, please see the accompanying DVD).

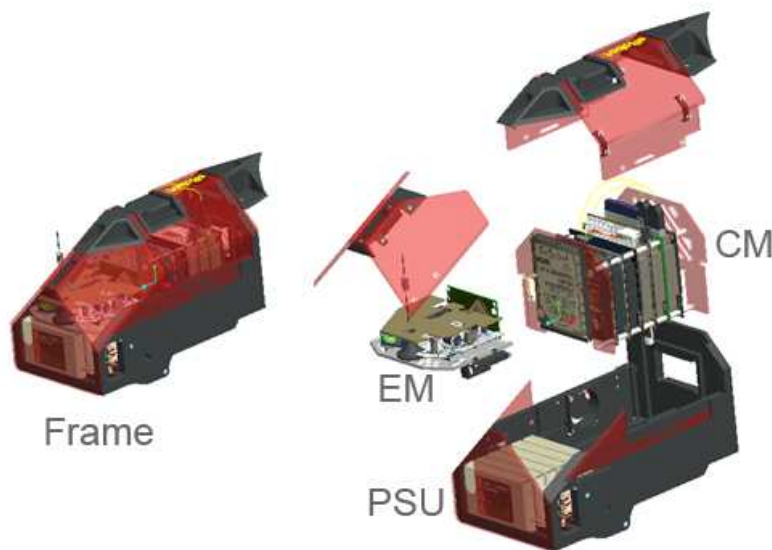


FIGURE 3-18: EXPLODED VIEW OF FRAME

As the central module of the entire vehicle, the frame was required to house all the necessary electronics and power supplies for the add-on modules. Specifically, this comprised the **P**ower **S**upply **U**nit (**PSU**), the **E**lectronics **M**odule (**EM**) and the **C**omputing **M**odule (**CM**). Also visible in the above image are the canopy sections, which served both to protect the internals of the vehicle and accommodate the GPS Active Antenna (in the rear canopy unit) to ensure the uBlox had an unobstructed sky-view.

Assembly and disassembly operations are crucial in a constantly-evolving development project. As such, the **CM** and **EM** were designed to be easily extractable. The CM slides into grooves machined into the frame, while the EM is fastened and unfastened by means of 4 easily accessible hex-bolts.

HDPE is relatively dense, and therefore various weight-saving features were incorporated into the design; however care had to be taken to ensure that the frame still had the required rigidity to hold the entire vehicle together.

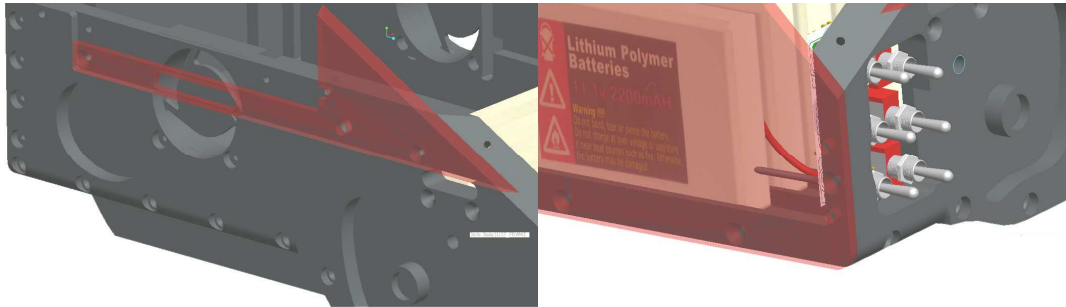


FIGURE 3-19: FRAME WEIGHT REDUCTION (LEFT) AND BATTERY INSERTS (RIGHT)

Shown in the left panel of **Figure 3-19** are some of the weight-saving insets that were machined in to reduce the overall weight of the frame. The right panel shows the PSU with its associated switches. These **Single-Pole Double-Throw (SPDT)** centre-off switches allowed for each battery to have three modes: On, Off and Recharge, allowing for the batteries to be replenished from an external charger without having to remove the module.

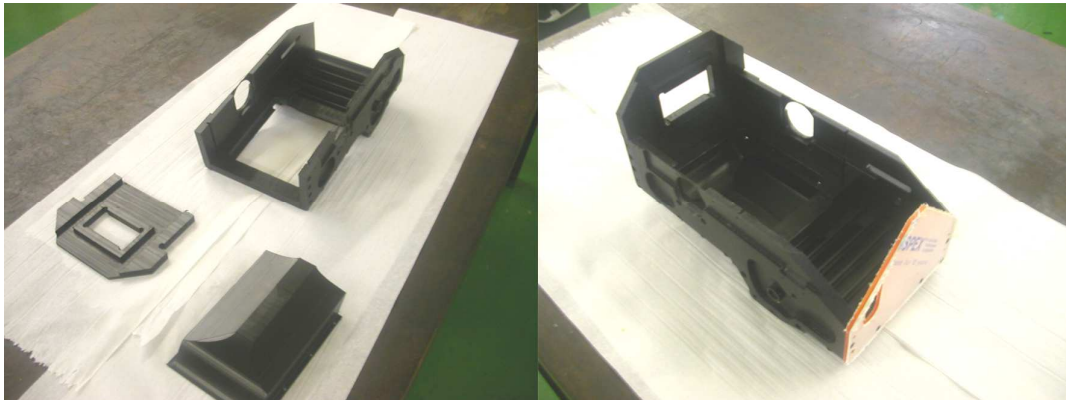


FIGURE 3-20: FRAME: PARTIALLY ASSEMBLED (LEFT) AND FULLY ASSEMBLED (RIGHT)

**Figure 3-20** shows the frame in various stages of assembly. Visible in the left image is the partially assembled frame with the rear brace and the bottom cover yet to be assembled. The right image shows the assembled unit, with the protective plastic layer still covering the Perspex bulkhead.

Also visible in the images are the circular openings for the cooling fans. These fans were required to regulate the temperature of the on-board electronics and were designed in such a way that air was drawn over the motor casings providing simultaneous cooling for the drive units.

## TAIL UNIT

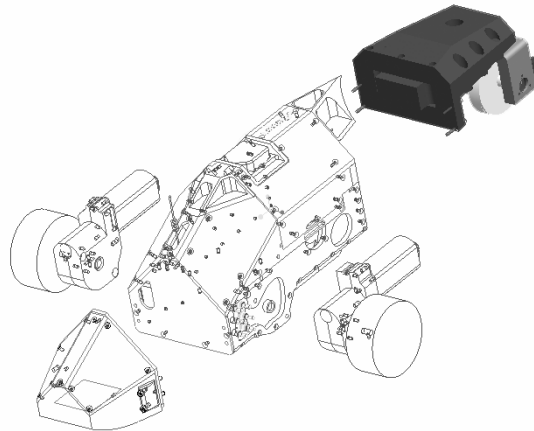


FIGURE 3-21: TAIL UNIT

In order to overcome the difficulties of the previous prototype, the drive configuration was modified from 4 to 3, with the rear wheel being a “jockey” wheel. The function of the **Tail Unit (TU)** was to allow the jockey wheel to rotate completely around its axis, allowing the robot to be driven forwards and backwards with equal ease.

As with all of the modules, design of the TU had to allow for the fact that other modules could be attached, and therefore should not dictate design requirements specific to its needs. Therefore, a slot and four 3mm bolts provide a standardised interface for securing whatever further modules may be attached.

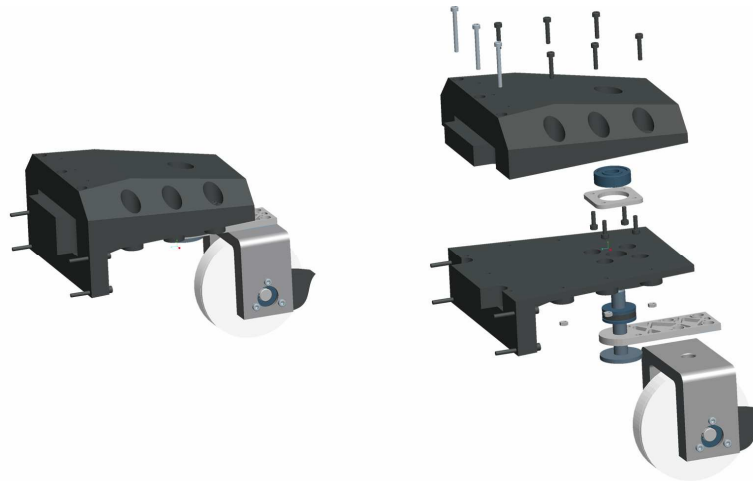


FIGURE 3-22: REAR (LEFT) AND EXPLODED (RIGHT)

As can be seen in **Figure 3-22**, the unit is mainly an assembly of two members, a top and bottom section which bear the structural load. The jockey wheel itself runs on a double bearing set. The top bearing is a conventional deep-groove bearing, while the bottom one is a thrust bearing.



The top and bottom members are fastened together by means of an array of nine 3mm hex-bolts, ensuring structural rigidity.

As the rear's capacity to handle load was of primary concern, a basic **Finite Element Analysis (FEA)** was conducted on the assembly, to ensure it would not deform substantially under load.

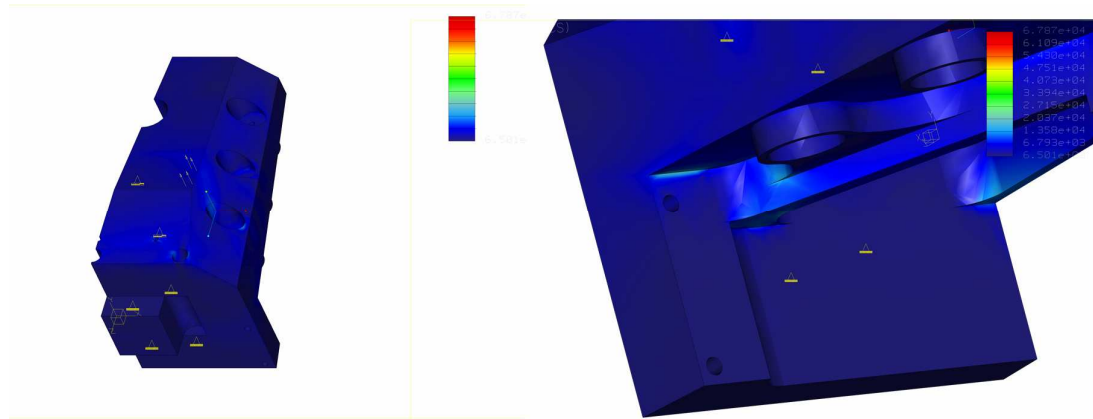


FIGURE 3-23: FINITE ELEMENT ANALYSIS

**Figure 3-23** gives a graphical representation of the analysis, and the maximum deflection of the shaft under load was only 2 millimetres, which was deemed acceptable.

A uniformly distributed load of 10 kilograms was placed on the internal bearing recess of the lower section. This was 125% of the design weight of the entire robot, leaving a large safety factor. The resultant maximum von-Mises stress was 1.9MPa, and with the yield strength of HDPE being approx 25MPa, there was a substantial safety factor for the assembly. In the above figure, the red gradient corresponds to 2.0 MPa, whilst blue is unstressed.

This led to the development of the machining models and the production of the required G-code for the CNC. Both sections were fabricated from solid blocks of HDPE. In both cases multiple machining operations were required, more for the top section (5 as opposed to 3 for the bottom section).

One major difficulty in the fabrication of the tail unit was the hitch sub-assembly. In the initial trial design, the jockey wheel ran on two silver-steel half-shafts and mating hubs, and was covered in electrical shrink-tubing to allow for slippage. However this arrangement did not provide the wheel with continuous smooth rotation, due to constant misalignment of the half shafts. This meant that the magnetic disc itself would have to be modified to allow a shaft to pass through. Machining of the shaft hole was a delicate procedure as the magnets themselves were very brittle; however Mr. Glen Newins of the Mech. Eng. workshop did an excellent job.

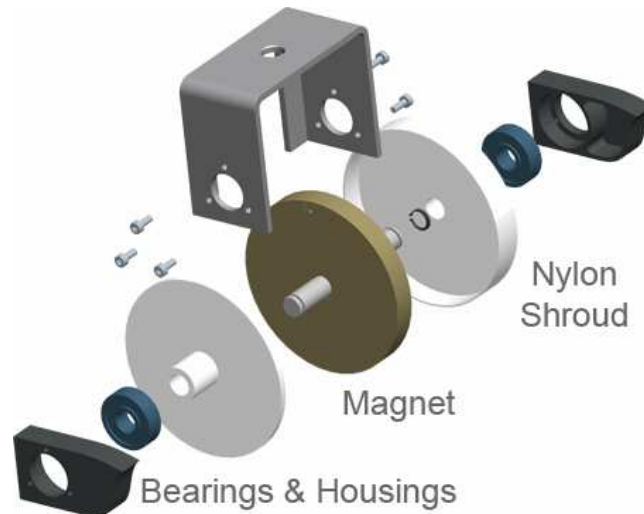


FIGURE 3-24: HITCH: EXPLODED

**Figure 3-24** shows the final design. The magnet accommodates a solid aluminium shaft (to prevent channelling of the magnetic flux into the bearings causing a reduction in operating life) and is encompassed by a nylon shroud. The entire sub-assembly, including the bearings and housing, is attached to the aluminium hitch by means of six 3mm hex bolts.

Shown in **Figure 3-25** are the two main elements of the tail unit during manufacture:

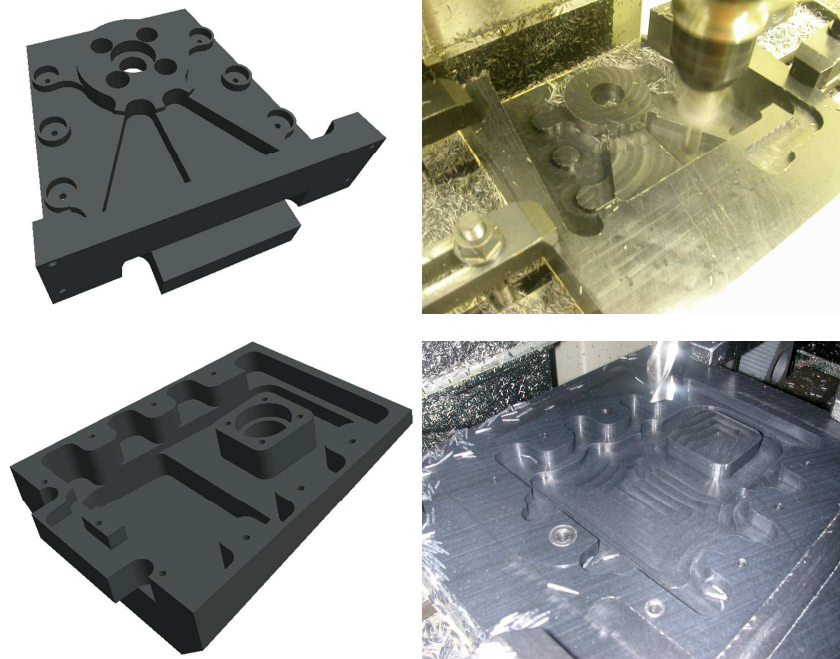


FIGURE 3-25: MACHINING OF TAIL UNIT COMPONENTS

In total, the fabrication of the final drive units took over 10 hours, with 12 individual machining operations and one combined operation. The structural

stiffness of the assembly was excellent, and the unit itself was aesthetically pleasing.



FIGURE 3-26: TAIL UNIT ASSEMBLY

**Figure 3-26** above shows various shots of the tail unit in assembly. The ribs visible in both the centre and left frames of **Figure 3-26** were inserted into the design after the FEA analysis during the design process showed excessive deflection of the assembly under load.

#### **PAYLOAD BAY**

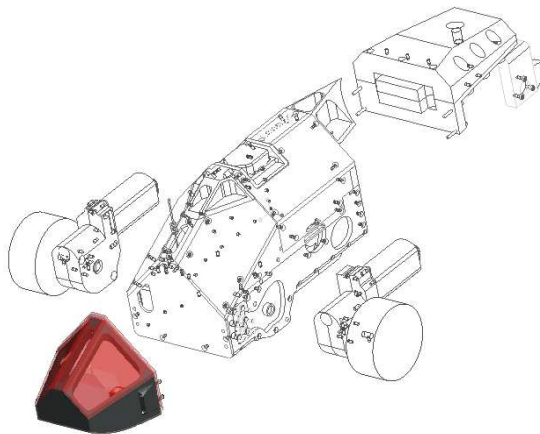


FIGURE 3-27: PAYLOAD BAY

As the name suggests, the payload bay is responsible for accommodating the NDE/inspection equipment for the vehicle. The modular design of all the sections allows for the replacement of one inspection module for another with minimal effort.

For this test vehicle, a FireWire<sup>®</sup> camera was used to capture images of the underlying surface, to allow for post-examination. This particular camera, a Fire-i<sup>®</sup> camera was capable of capturing a 640 pixel x 480 pixel stream at 30 fps in video mode. Although more suited to streaming media, the camera was designed to be used in still-capture mode.



FIGURE 3-28: FRONT SHOWING FIREWIRE CAMERA

**Figure 3-28** shows the Fire-i and its associated connector. Also visible in the image are the weight-reducing volumes that were milled out to keep the weight of the bay to a minimum.

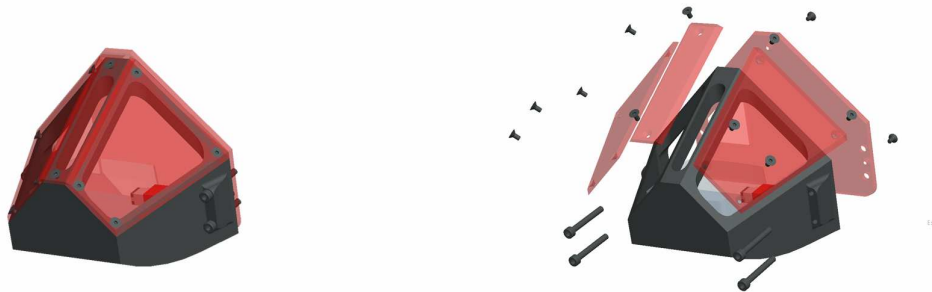


FIGURE 3-29: FRONT (LEFT) AND EXPLODED VIEW (RIGHT)

The bay is of single-piece construction, and required 18 operations and a total machining time of approximately 6 hours to complete (not including set-up and programming). Initially, the bay was going to be constructed of several interlocking sections (as the Hercus CNC lacked the work envelope to fabricate it out of one solid section) however the Department of Mechanical Engineering took delivery of a bigger CNC in late October 2006.

This allowed the author to re-design the bay to take advantage of the greater work-volume of the bigger CNC. As such, the bay is more rigid and required fewer fasteners than the comparative multi-piece design.



FIGURE 3-30: FRONT: MACHINING

Shown in **Figure 3-30** is the single-piece bay as designed (left) and being machined on the CNC (right). The operation in progress is the smoothing of the faceted edges using a ball-nose cutter. In order to obtain a quality surface finish, the cutter is stepping along at 0.3mm intervals, and as such constituted one of the most time-intensive operations.

#### **MANUFACTURE & ASSEMBLY**

Manufacture of the platform was accomplished almost exclusively on the CNC machinery of the Department of Mechanical Engineering. Design for CNC manufacture allowed for more complex geometry than would otherwise be possible. In addition, once the author had shown proficiency in the CNC process, he was free to use the machines at any time. This allowed for a much greater scope of independence than would otherwise be possible.

An overview of the design process from concept to construction for one of the parts that was machined (there were over 30 in total) is given below.

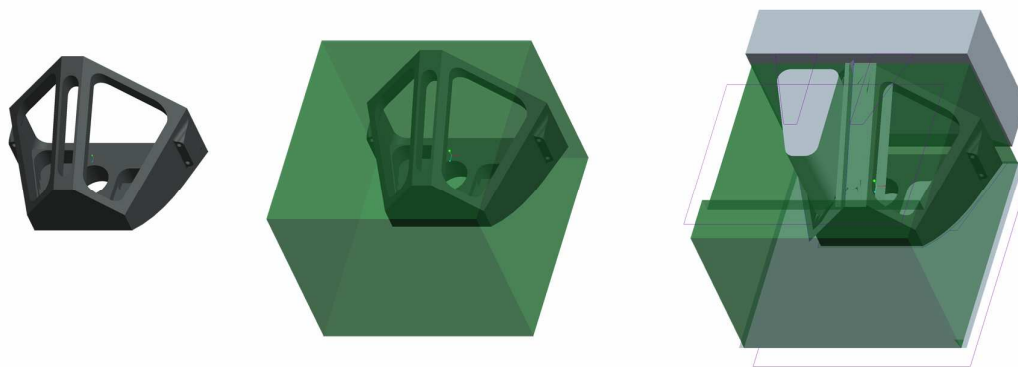


FIGURE 3-31: PART, WORK-PIECE, MANUFACTURING MODEL

On the left of **Figure 3-31** is part to be manufactured once design has been completed in Pro/ENGINEER. Pro/ENGINEER is a parametric 3-dimensional **CAD**

(**C**omputer **A**ided **D**esign) software package widely used in industry. Boeing, Airbus and John Deere are some of the biggest users of Pro/ENGINEER software.

It is, of course, very important to design with manufacture in mind, specifically with how the component is to be located and held in the CNC machine. This particular component (the nose section of the **P**ayload **M**odule (**PM**)) required no less than 12 machining operations for a sum total of 24 NC sequences.

Assembly of the **w**orkpiece and component in the Pro/MANUFACTURE environment is the next step in the process. Pro/MANUFACTURE is an add-on multi-axis prismatic machining module that allows Pro/ENGINEER designs to be fabricated on a CNC machine.

The workpiece represents the stock that is going to be machined to leave the final part. This step is optional, however omitting the workpiece can lead to visualisation difficulties of how the component actually looks when the process gets complicated (for the operator, not the software).

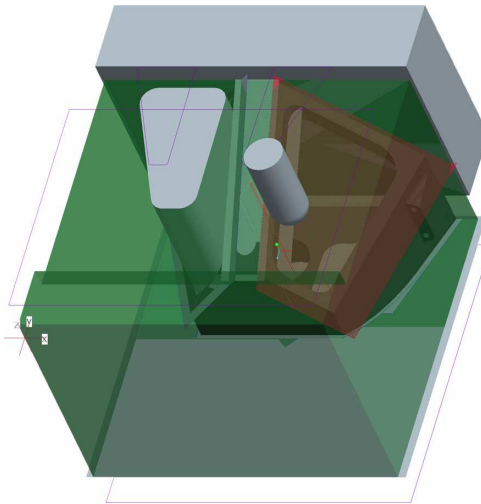


FIGURE 3-32: TOOL-PATH GENERATION & CHECK

Pro/MANUFACTURE allows for several ways of checking the tool-paths generated for the manufacturing geometry. There is an on-screen check, useful for quick debugging, as well as more advanced modules such as Vericut<sup>®</sup>, which gives other capabilities such as gouge-checking (checking to see whether the tool rapids incorrectly into any part of the job). The parametric nature of Pro/ENGINEER (the ability to modify any attributes of a feature after it has been created) means that modification of tool paths is relatively easy.

Once the tool-paths are seen to be correct, the machine-specific post-processor is invoked. With the help of Gary Phipson of Automated Reasoning (local distributors of Pro/ENGINEER software), the initial post-processor was developed for the



Hercus<sup>®</sup> CNC Milling Centre (which previously had relied on 2D CAD software of limited capacity).

At this point it should be noted that mechanical design of the robot had to take into account the limited work-envelope of the Hercus. The introduction of the new Syntech CNC in late November had a minimal effect on the project.

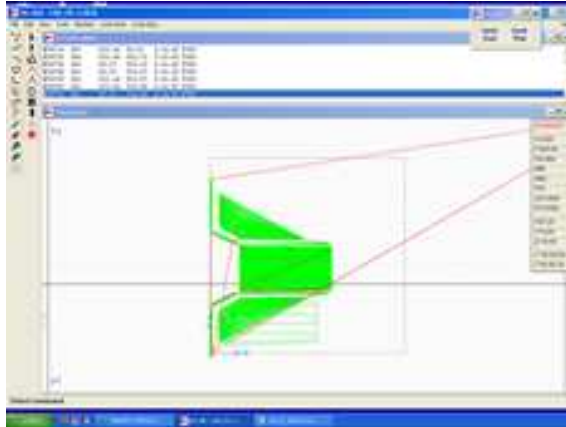


FIGURE 3-33: G-CODE SIMULATION

The machine G-code generated by the post-processor was checked on a simulator before it was taken to the machine. This allowed for last-minute error-checking to prevent errant code from causing an expensive mishap later on. Shown below is a chronological cross-section of the CNC machining process as it matured:



FIGURE 3-34: BASIC MANUFACTURE

Shown above in **Figure 3-34** are some of the earlier machining attempts. The leftmost image was a failed attempt at the Tail Unit top section. Centre and right are images of the final unit.

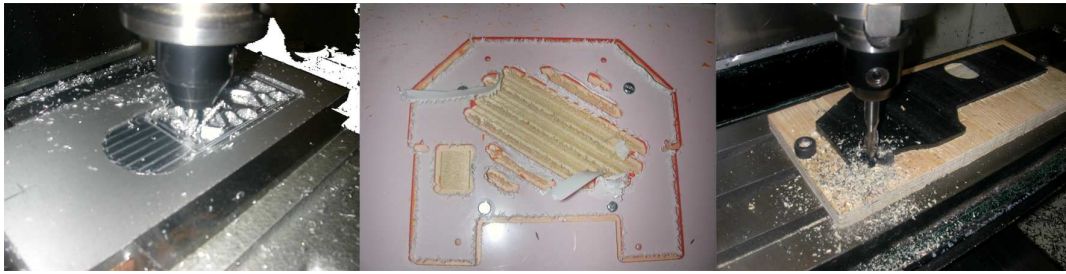


FIGURE 3-35: DIFFERENT MATERIALS & TECHNIQUES

Various materials were used in the project, all providing different challenges. The aluminium tail hinge is shown on the left, with one of the Perspex<sup>®</sup> **Computing Module (CM)** supports shown in the centre. Manufacture of the side panels of the frame was testing, in that accurate locating of the part (to perform the reverse-side machining operations) was tricky as the component had complex and non-perpendicular geometry. This particular problem was solved by machining the **negative** shape of the part into a block of wood, and pressing the component in.



FIGURE 3-36: MULTI-PROCESS MACHINING

Some components had to undergo multiple machining operations. The drive units were composed of two individual components (one of which is shown on the left in **Figure 3-36**) which required machining on both the top and bottom surfaces. These were then assembled together and the bearing recesses and locating holes were machined in (**Figure 3-36**, centre). Finally an aesthetically appealing round was machined in with a ball-nose cutter (**Figure 3-36**, right).





FIGURE 3-37: EXTENDED ONE-PIECE MACHINING

With the introduction of the larger CNC machine, it became possible to perform more complex machining tasks. The Payload Bay frame has been discussed previously, machining sequences from which are shown in **Figure 3-37** above. On the left is the roughing sequence (identifiable by the contour-like ridges left behind), with the surfacing sequence on the right hand side.



FIGURE 3-38: INITIAL PROTOTYPES (LEFT) AND FINAL COMPONENTS (RIGHT)

Finally, **Figure 3-38** shows the differences in the frame sections of the initial prototype (left) and the final sections (right).

### 3.3 Electrical Design

#### DESIGN ENVELOPE

As design for all individual modules was performed concurrently, a design volume or **envelope** had to be allocated for the required low-level electronics. It was uncertain at the time of allocation how much space would be required for the electronics module. However, it was known that the module would be required to:

1. Dissipate the heat generated by the motor-driver circuitry
2. Interface with the uBlox **G**lobal **P**ositioning **S**ystem unit
3. Electrically and physically separate the computing and electronic circuitry

Use of Pro/ENGINEER and Eagle CAD (a freely available **E**lectrical **C**omputer **A**ided **D**esign (**ECAD**) package) allowed for the design of boards that were electronically correct, in addition to being of the right form to integrate seamlessly with the mechanical design.

#### DESIGN OUTLINE

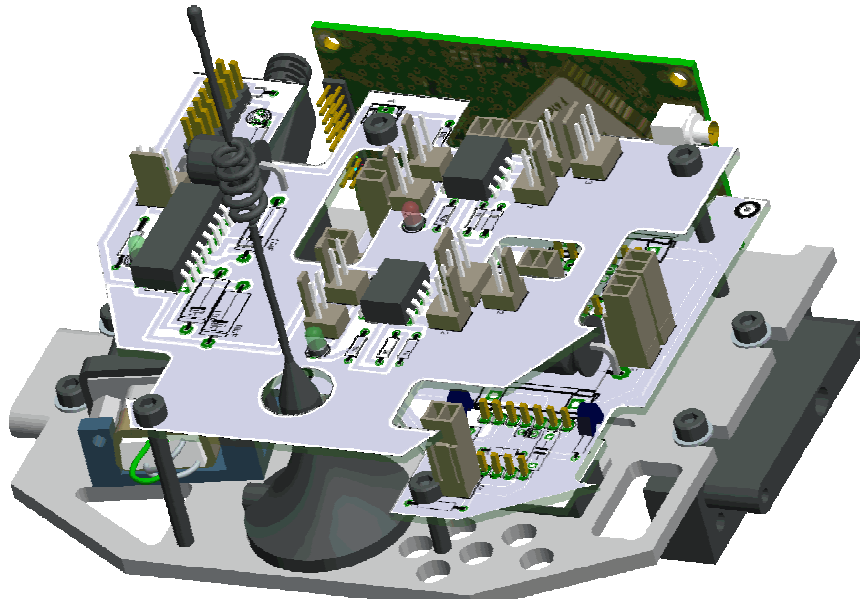


FIGURE 3-39: **ELECTRONICS MODULE (EM)**

From the allocated design volume it was possible to segment the electrical components into layers, a short description of which is given below (moving from the bottom layer upwards):

#### **FIRST LAYER – POWER CIRCUITRY**

This layer was responsible for isolating a motor-control signal from the PC104 **C**omputing **M**odule (**CM**), and accommodating necessary electronics for the drive motors.

## SECOND LAYER – GPS INTERFACING CIRCUITRY AND SPEED CONTROL

Use of the GPS board required providing it with supply voltages, as well as a reduced voltage for antenna gain-switching, and connectors to the on-board serial ports. In addition the layer would accommodate the interface circuitry for the motor thermal and speed sensors.

## THIRD LAYER – ADDITIONAL CONTROL MODULES

The third layer was designated for any other control modules that would be needed during the course of the project.

## LOWER BOARD

As mentioned previously, the purpose of the lower board was to isolate a **P**ulse-**W**idth **M**odulated signal from the **CM** and deliver an amplified PWM signal (i.e. from 0V to 5V) to the input of the LMD18200 H-Bridge driver chips.

For this board the H-bridge chips are mounted on the solder side. This was because the tabs of the H-bridge had to be in thermal contact with the underlying aluminium base. In this case, insets were machined into the base during manufacture, to allow for a greater heat transfer from the H-bridge to the base.

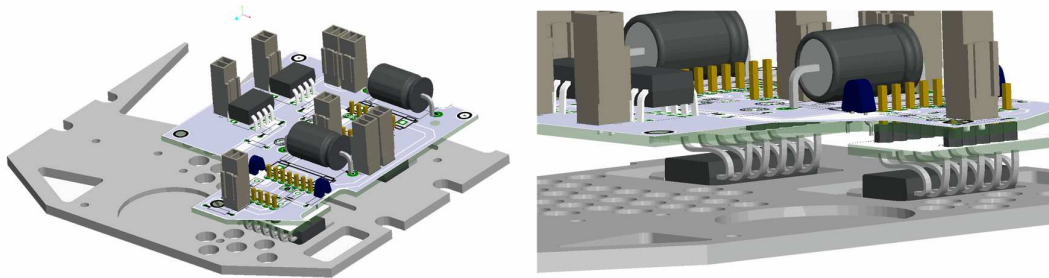


FIGURE 3-40: BOTTOM BOARD (LEFT) AND H-BRIDGE RECESSES (RIGHT)

## LAYOUT

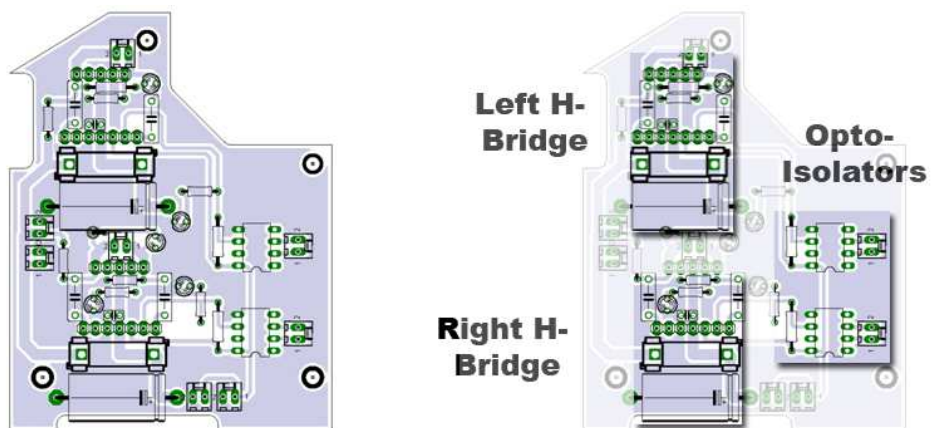


FIGURE 3-41: ELECTRONICS: H-BRIDGE INSETS (LEFT) AND uBLOX GPS (RIGHT)

Several revisions were made during the course of the project. The LMD18200 Motor Driver Chips have an integrated thermal protection circuit, which meant that once the chip's temperature exceeds 158°C, the outputs are no longer driven.

Cooling was therefore vital, and as such mounting on the underlying aluminium base was critical. This led to the initial (overly optimistic) design as shown below:

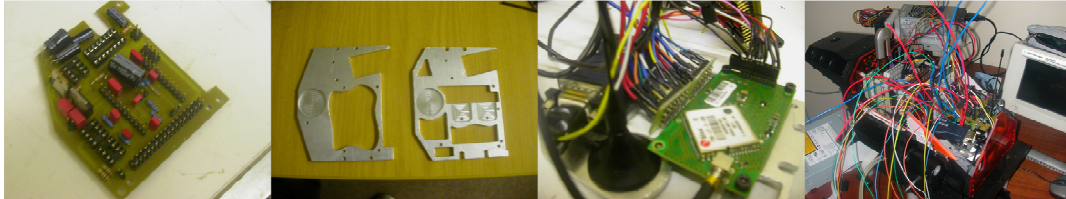


FIGURE 3-42: INITIAL BOARD

The initial design allowed for each motor-driver chip to be sunk into the aluminium base, affording excellent thermal contact to the aluminium. Ultimately it proved to be unworkable, as it required each lead of the 11-pin H-bridge to be routed by means of a wire onto the board itself. This led to an overwhelming number of connections as can be seen from the extreme right panel of **Figure 3-42** (dubbed unkindly "the Porcupine" by some bystanders).

As a result of this, the design was revised to incorporate the chips in an inverted position on the solder-side of the board, which is not unusual but can lead to some soldering difficulties.

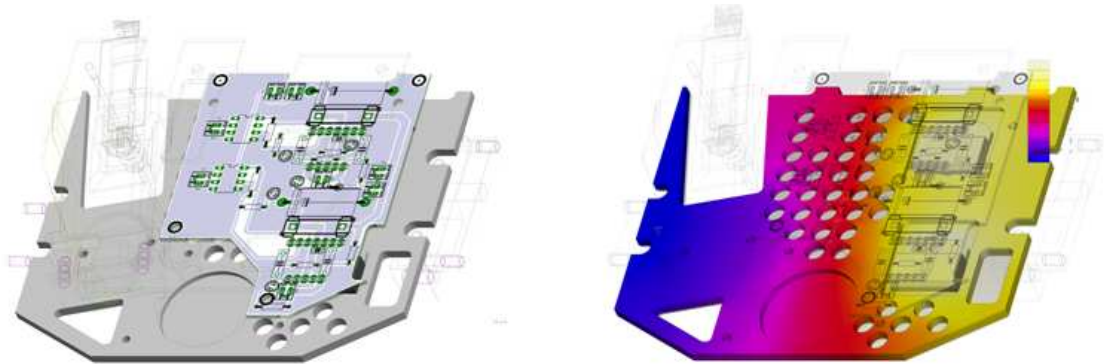


FIGURE 3-43: THERMAL PLOT

Shown in **Figure 3-43** above is a thermal plot of the heat flow through the board. Clearly visible on the right-hand plot are the high-intensity areas corresponding to the H-bridge heat tabs. The use of Finite Element Analysis software in this way allowed for a visualisation of the cooling capacity of the different aluminium base designs. In this analysis, the blue region corresponds to the ambient temperature (assumed to be 25°C) with the yellow sections corresponding to the thermal maximums of the H-Bridges (i.e. 158°C).



## CENTRE BOARD

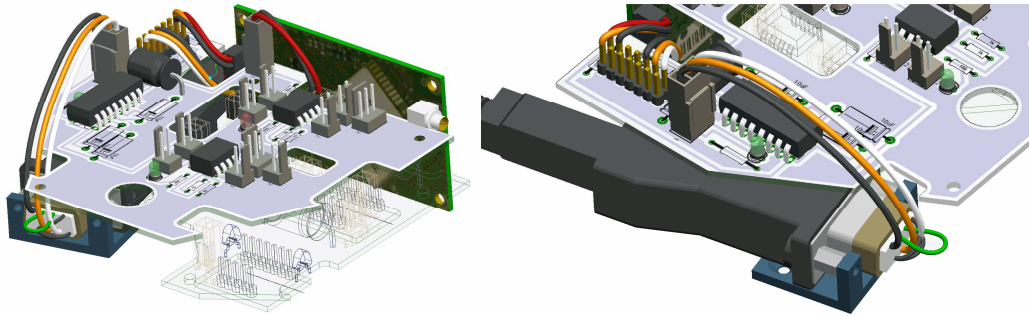


FIGURE 3-44: CENTRE BOARD (LEFT) AND GPS INTERFACE (RIGHT)

Interfacing with the uBlox<sup>®</sup> GPS module was the primary requirement for the second (centre) board.

Due to the stacking procedure on the PC/104, both serial ports had to be sacrificed (i.e. their dedicated **Interrupt Requests** or IRQ's were required by the other boards), and so therefore a USB-to-serial converter was integrated in to the system (visible in **Figure 3-44**). A USB-to-TTL converter would have been more appropriate, as the logic levels undergoes a shift from USB to RS232 to serial; however a USB-to-serial converter was easier to obtain.

This required the use of a level shifter, as RS232 voltages operate from -3V to -15V (logic "high") and 3V to 15V (logic "low"). TTL and CMOS logic requires 0V to 5V, and so a MAX232 transceiver chip was used. The MAX232 is a **full-duplex** chip, allowing concurrent transmission and reception.

## LAYOUT

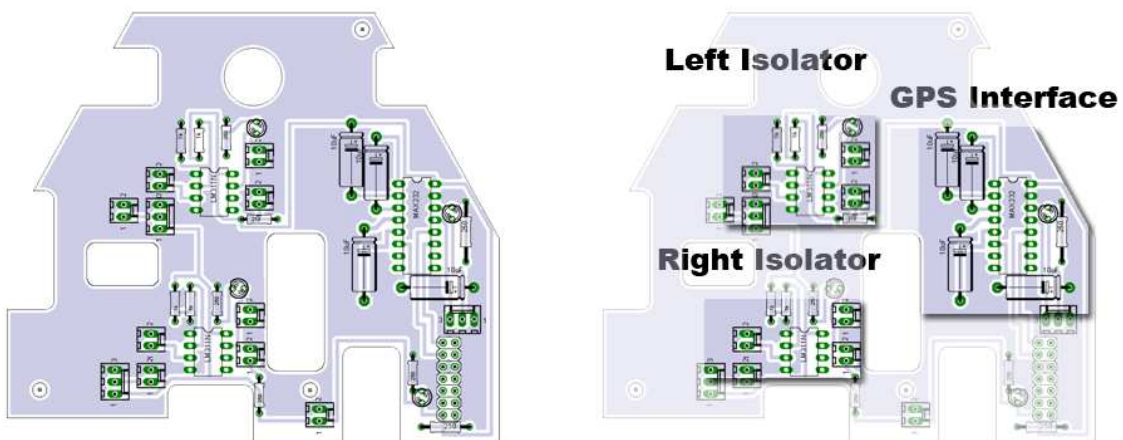


FIGURE 3-45: CENTRE BOARD

The unusual geometry of the board is due to the design methodology used. As the base board was of primary concern to the motion capabilities of the robot, the

centre board was designed to allow access to all the Molex<sup>®</sup> connectors of the lower board.

Design of the boards was an iterative cycle between Pro/ENGINEER and Eagle CAD. A board outline was generated in Pro/ENGINEER and exported as a .dxf file. This was converted (by means of a script generator) into a sketch on the dimension layer of Eagle's Board editor.

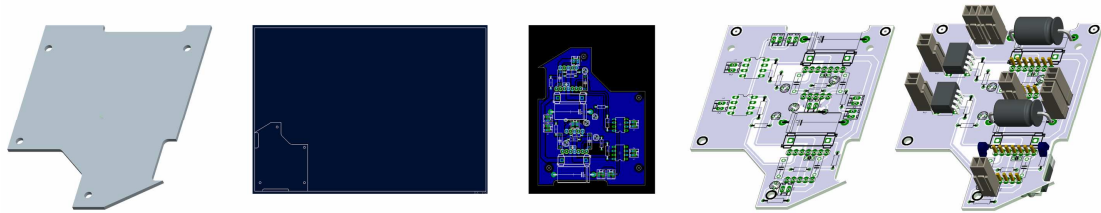


FIGURE 3-46: PART->.DXF->.BRD->.TIF ->ASSEMBLY

All of the required tracks and pin placements were performed, taking care not to violate the perimeter of the board. From the board editor, a .tif file was exported showing all the component placements. The .tif file was imported back into Pro/ENGINEER, and converted into a texture. This texture was then mapped onto the initially generated board design, and then populated with 3D models of the components.

Design in this method was sometimes laborious, however it ensured that there were a minimum of interferences when the module was assembled. Provision could also be made for the minimum bend-radii of all the wire connectors, ensuring that thick wires would not prevent the unit being assembled.

#### **DIFFERENTIAL GLOBAL POSITIONING SYSTEM (DGPS) CARD**

In order to obtain accurate DGPS data, a transportable PC/104 node was developed as a dedicated GPS-streaming server. This lightweight unit's sole function was the streaming of GPS data back to the main server in order to calculate DGPS data. A full explanation of the system architecture can be found in the **Communication, Navigation & Control** section. Shown overleaf in **Figure 3-47** is the board as designed in Eagle CAD:

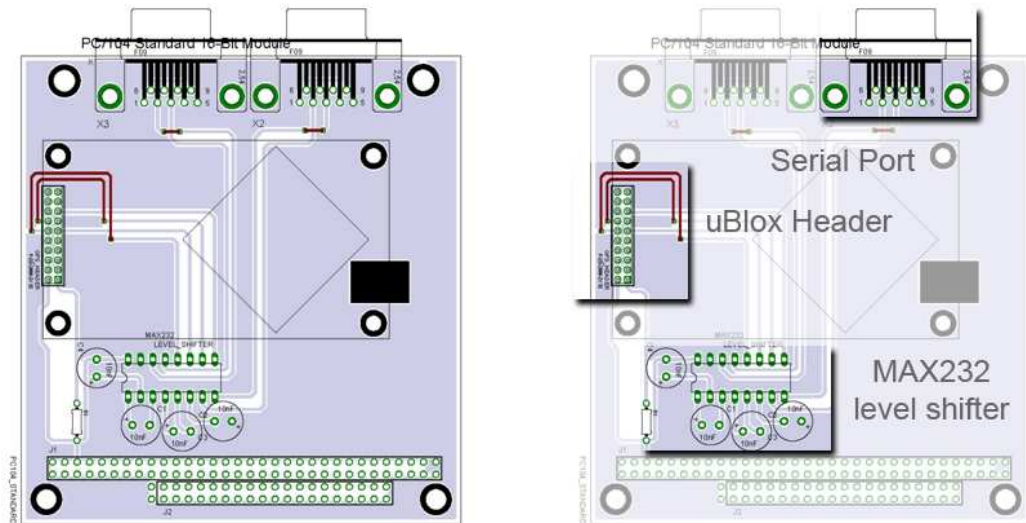


FIGURE 3-47: DGPS BOARD

The board was designed to be stackable on a standard PC/104 bus. The uBlox GPS unit used in the project has two serial outputs, and these are accommodated on the board by means of two DB9 serial headers, visible in **Figure 3-47**.

#### BOARD MANUFACTURE & ASSEMBLY

Fabricating boards used to be an intensive process, both financially and with respect to time. As the **EM** required exacting shapes and layouts in order to be able to integrate with the rest of the robot, it was decided to attempt to fabricate the boards on the Departments Hercus CNC 3-Axis Mill.

Documentation on the mill states the accuracy of the slides to be 0.01mm. This corresponds to a board accuracy of approximately 3mils (not to be confused, as the author initially was, with the metric slang for millimetres. 1 mil in board fabrication parlance is 1/1000<sup>th</sup> of an inch.)

On consultation with Cadshop, a Pretoria based CNC board milling specialist, a variety of milling tools were purchased. The width of the tools ranged from 0.4mm (15 mils) to 0.7mm (27 mils). The tools shipped were long series, and it was obvious that some sort of tool adaptor would have to be constructed to prevent tools failing repeatedly at the neck.

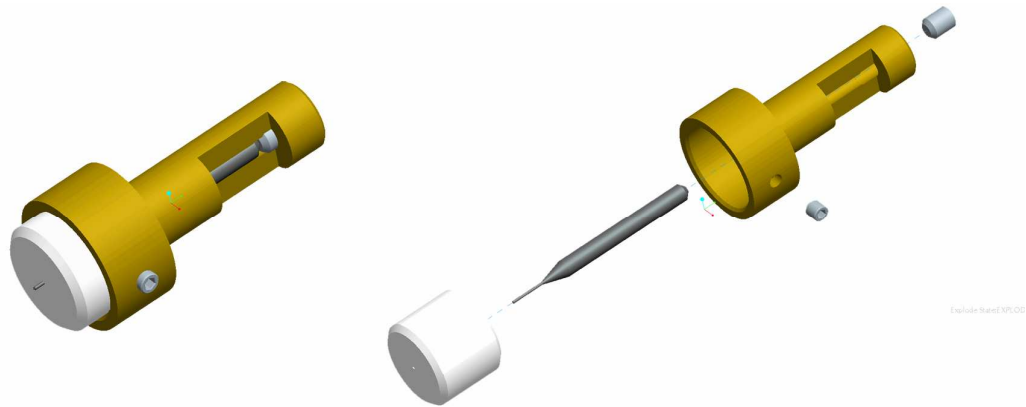


FIGURE 3-48: TOOL SUPPORT AND ADAPTOR

This meant that the minimum spacing (track/track, track/via, etc) was 27 mils. A set of design rules was constructed in Eagle CAD to ensure that this was not violated. However, 27mil spacing meant that tracks could not be routed between IC leads. This, in conjunction with the fact that only a single-sided board could be fabricated with any accuracy, gave rise to a crowded first board.

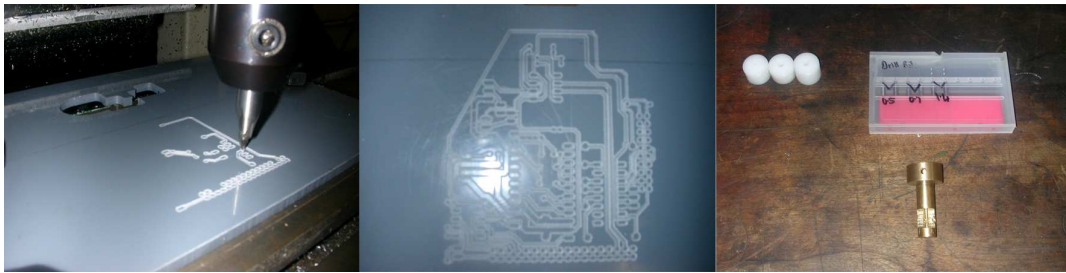


FIGURE 3-49: BOARD MANUFACTURE: TESTING

Shown in **Figure 3-49** are the initial testing steps that were performed to see if in-house board fabrication was possible. An end-mill sharpened to a cone was the initial test-tool and as can be seen from the centre photograph the tracks (although very burred) can be easily discerned.

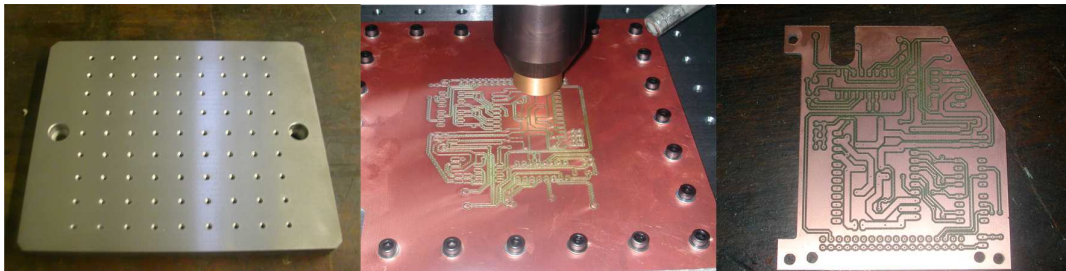


FIGURE 3-50: BOARD MANUFACTURE: PRODUCTION

In order to ensure that the board was completely flat when machined (as the blank PCB had a tendency to curl) a base plate was ground, then drilled on the CNC and tapped. This allowed for the board to be fastened by no less than twenty-six 3mm bolts, ensuring the board was uniformly flat.



## ASSEMBLY



FIGURE 3-51: ASSEMBLED BOTTOM BOARD

**Figure 3-51** shows the end result of the manufacture, with the components soldered in and the H-Bridges on the solder side ready for incorporation into the electronics module.

Nearing the end of the project, it became possible to use the Department of Electrical Engineering's LPKF PCB Milling Machine. All boards after the initial drive board were then manufactured on the LPKF, allowing for tighter tolerances, in the order of 10mils.

In **Figure 3-52** the base and bottom board of the **EM** assembly can be seen, as compared to the initial board. On the right of **Figure 3-52** the board is being installed into the dedicated electronics bay of the robot.

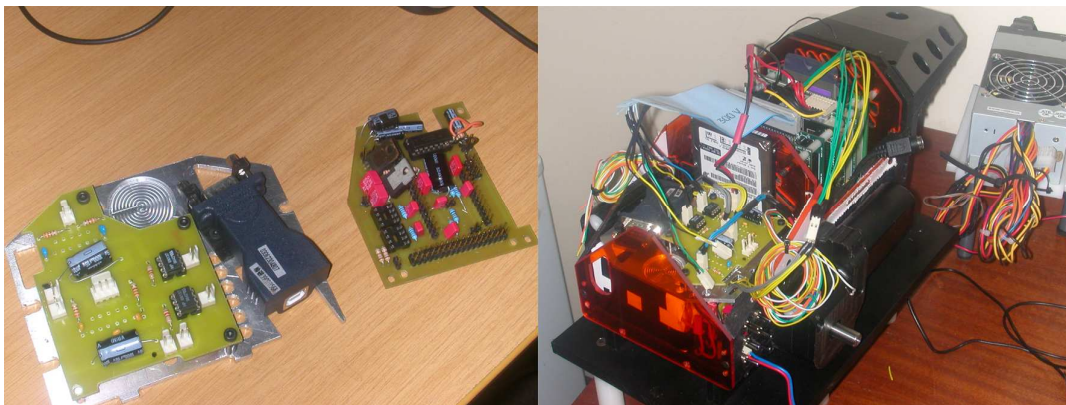


FIGURE 3-52: BOARD ASSEMBLED (LEFT) AND INSTALLED IN ROBOT (RIGHT)

## 4. COMMUNICATION, NAVIGATION & CONTROL

### 4.1 Embedded Computing

Central control and communication for the robot platform was achieved with use of an embedded PC/104 stack. The PC/104 format is a particular computing standard that promotes stacking – that is, various modules can be stacked progressively onto each other adding capabilities to the base motherboard, and is very common in **A**utomated **T**eller **M**achine's (**ATM**'s) and other high-intensive embedded applications.

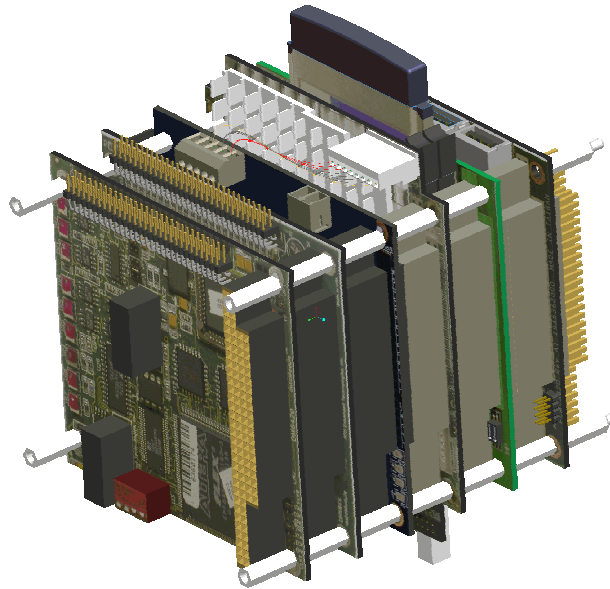


FIGURE 4-1: THE PC/104 "STACK" (RENDERED)

Shown above is a Pro/ENGINEER rendering of the PC/104 stack. The stack itself is a mixture of **RTD Embedded Technologies** Digital I/O boards, and **Advantech** conventional PC/104 and PC/104-Plus components.

#### HARDWARE DESCRIPTION

As mentioned previously, the PC/104 architecture is very modular and used for a variety of embedded tasks where robustness and size is important. Amongst other things, PC/104's can be found in vending machines, medical instruments and industrial control systems. The system used in this case is also PC/104-Plus compatible, meaning both ISA and PCI buses are available.

More information on the architecture can be found at the PC/104 Embedded Consortium's website. [29]

## PCM-3370 & POWER SUPPLY

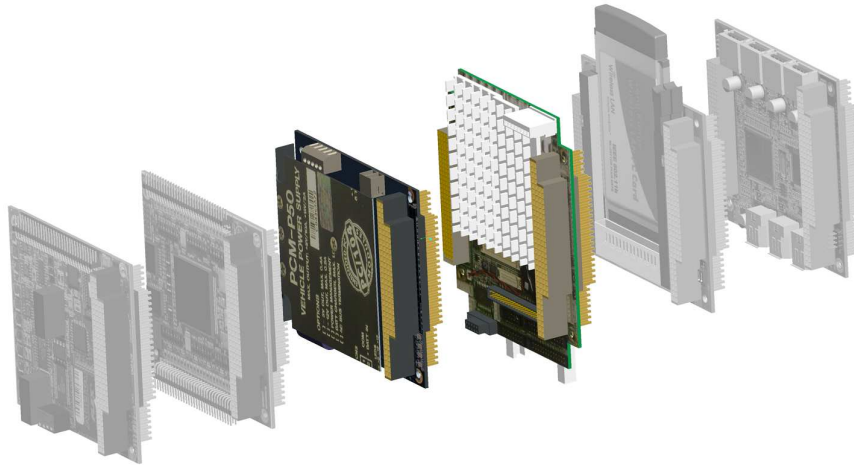


FIGURE 4-2: ADVANTECH PCM3370

Each PC/104 unit is commonly referred to as a “stack”. Each stack must have a motherboard and **C**entral **P**rocessing **U**nit (**CPU**), which together is commonly referred to as a **S**ingle-**B**oard **C**omputer (**SBC**). This SBC was an Advantech PCM-3370, running an **U**ltra-**L**ow **V**oltage (**ULV**) Celeron® 650 processor, with 512Megabytes of RAM. The board accommodated both PC/104 and PC/104-*Plus* connectors, allowing the addition of the **R**eaL **T**ime **D**evice (**RTD**) data acquisition boards and the USB and **PCMCIA** expansion boards. In its factory-configuration, the PCM-3370 had 3 free interrupts available for peripheral devices, however the **B**asic **I**nput-**O**utput **S**ystem (**BIOS**) allowed for peripherals (such as the on-board USB, serial ports, Ethernet port and so on) to be disabled, freeing up resources.

The PCM-3370 was a power-hungry unit, requiring two 11.1**V**olt Lithium-Ion batteries configured in parallel in order to provide sufficient power to the unit. In the cases where the battery voltage started to drop (and were not capable of providing 3 Amps peak current) the unit would exhibit erratic boot behaviour.

A 50W PCM-P50 power supply regulated the power from the batteries and provided +12V, +5V, ground, -5V and -12V supplies. Unfortunately, the power supply did not have a through-header for the PC/104-*Plus* bus, which required the stack to be assembled in a certain order.

## DM6420

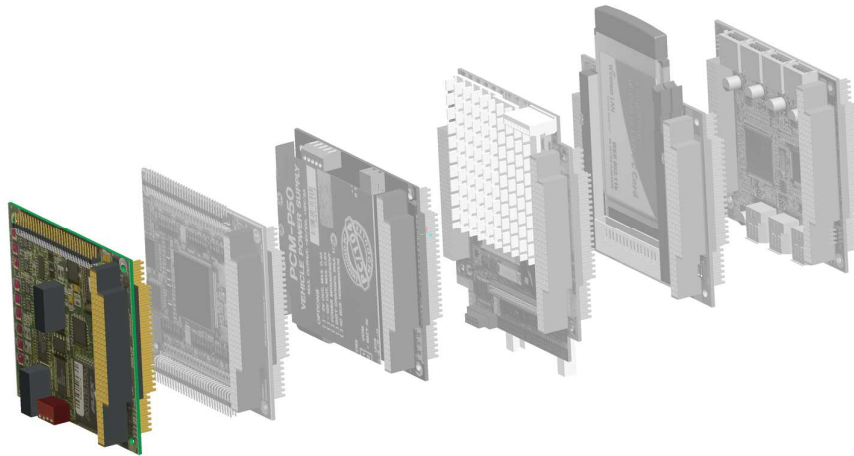


FIGURE 4-3: RTD DM6420

**Real Time Devices (RTD)** are manufacturers of a large variety of “computer modules and systems for Industrial and Aerospace Applications” [30]. In particular they develop a large number of **Input/Output (IO)** devices in the PC/104 form factor. One of these boards that the Department possessed was a DM6420 Data Acquisition board, with 8 differential (16 single-ended) analogue input channels, a 12 bit **Analogue-to-Digital Converter (ADC)** and a host of timers and counters, all useful for sensor monitoring and sampling.

## DM6816

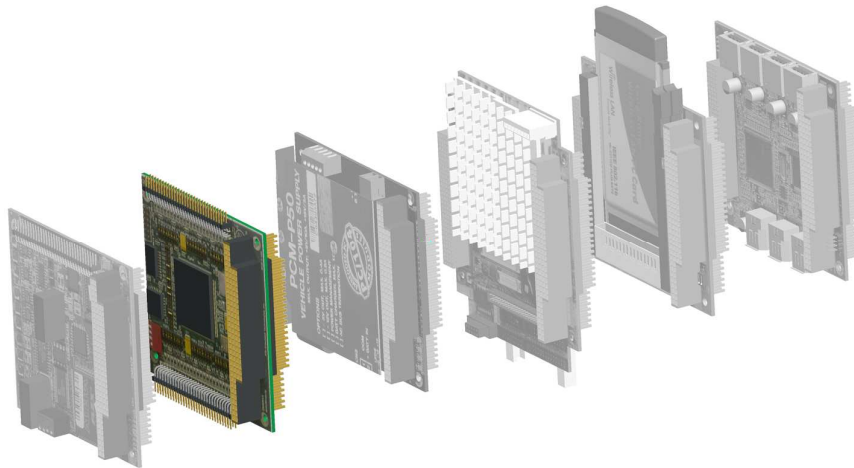


FIGURE 4-4: RTD DM6816

Also developed by RTD is the DM6816, which is a **Pulse Width Modulator (PWM)** and Digital I/O board. The DM6816 has 8 dedicated 8-bit PWM channels and 8 digital I/O ports, making it very useful for controlling motors.

## PCMCIA EXPANSION BOARD

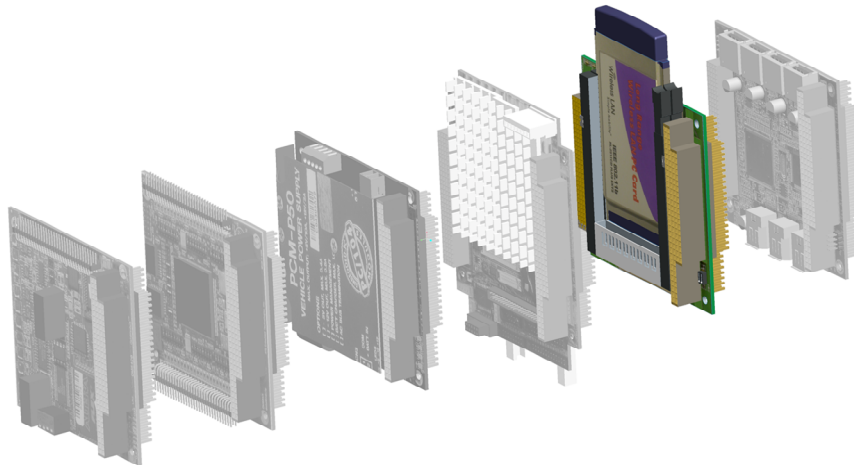


FIGURE 4-5: ADVANTECH PCMCIA EXPANSION CARD

Wireless networking capacity was provided by the PCMCIA expansion board, which had two slots for Type I/II/III or CardBus cards. In the case of eRobot, an 802.11g WiFi card was used. In conjunction with the booster aerial, the card had a rated working range of 1km. This was very optimistic, however as the network became unstable (excessive numbers of dropped packets) over 250 metres.

## IEE1394 FireWIRE®/USB 2.0 EXPANSION BOARD

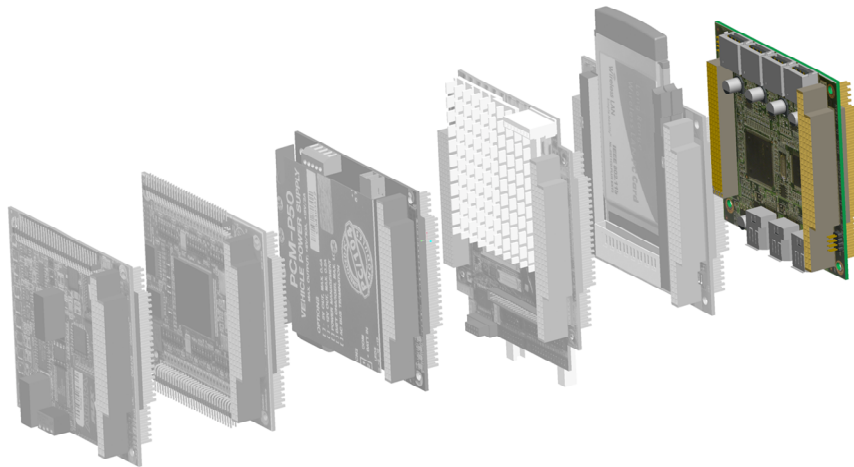


FIGURE 4-6: FIREWIRE®/USB 2.0 EXPANSION BOARD

As the PCM-3370 motherboard only had two USB 1.1 connections, an add-on expander board was used to provide 3 FireWire® ports and two USB 2.0 ports. However, the **usb-uhci** and **usb-ohci** Linux drivers would not allow peripheral access to **both** the on-board and the expansion board ports. Therefore the low-speed native USB 1.1 ports were sacrificed for the add-on USB-2.0 ports.



## OPERATING SYSTEMS

### eROBOT:



RedHat Linux was chosen as the operating system for the robot. This choice was made fairly early on in the development cycle, for a number of reasons.

Firstly, it was observed that the loading and unloading of drivers in Windows<sup>®</sup> 2000 was sometimes erratic. This may have been due to the way the device drivers were loaded (i.e. only when calls were made to the device driver). Also, nodes on

the wireless network had a nasty habit of displacing other nodes at random times (although in retrospect this may have been due to the **ad-hoc** architecture of the network).

Secondly, from the documentation on the two Digital I/O boards, RedHat Linux 9.0 (Shrike) was the most recent open-source platform for which development had been done. As most of the chipsets that were being used were common to standard PC's, compatibility for the rest of the PC/104 components was not an issue.

Although open-source RedHat has been discontinued (and has been re-named Fedora) RedHat 9.0 was still supported as a legacy build at UCT's Linux Enthusiast's Group (**LEG**) website [31].



### SERVER CLUSTER:

Ubuntu is a Debian-based Linux distribution that is rapidly becoming one of

the most popular flavours of Linux. Ubuntu was chosen for the servers as it is relatively easy to install and configure (compared to other more powerful but complex versions such as Slackware). Ubuntu has a very user-friendly package manager known as **apt**, and this in conjunction with an Ubuntu mirror hosted at the UCT LEG website greatly simplified the installation and configuration of software packages.



### DGPS Node:

The DGPS node was a minimalist PC/104 stack with Windows<sup>®</sup> 2000 as the **Operating System (OS)**. Use of the Windows<sup>®</sup> OS allowed access to a greater number of binaries (executable files) developed for GPS applications than

would otherwise have been possible with a Linux-only architecture. In addition the

incorporation of a Windows machine shows the compatibility of the system for a variety of operating systems.

## SOFTWARE

Use of existing programs and code allows for a quicker development-test cycle than would be possible if code was to be developed independently for every element of functionality.



FIGURE 4-7: SOFTWARE: GPSD, GPSDRIVE AND APACHE

As such, open-source software was utilised as much as was feasible to develop the system. An overview of some of the most pertinent software used is outlined below.

### GPSD

**gpsd** is an open source daemon that is capable of monitoring several GPS devices on a system and making the data available on TCP port 2947 [32]. This enabled the GPS data from the robot to be made available on the LAN.

### GPSDRIVE

**GpsDrive** is a “car (bike, ship, and plane) navigation system” [33]. GpsDrive is a Linux application that allows the plotting of a NMEA-compatible receiver on a scaleable map; however most importantly for the project it stores this data in an eXtensible Mark-up Language database (XML) file, making the data available for post-processing. GpsDrive makes use of Gpsd to access GPS devices.

### APACHE

**Apache** is an established open-source web-server developed at the Apache Software Foundation. Apache is an easy-to-use, highly configurable web server that supports Perl, Python, Tcl and PHP scripting [34].

Shown in **Figure 4-8** overleaf is a screenshot of the website developed for the robot (a full mirror of the website is available on the accompanying DVD).

Development of the website provided the author with experience in various aspects of Web design, including Cascading Style Sheets (CSS) for a more aesthetically pleasing site and Perl Common Gateway Interface (CGI) scripting for dynamic website content.

As one of the initial hopes for the system was that users would be able to view the robot data over the web in real-time, the implementation of a web server and a **MySQL** database on the vehicle meant that the lead time to develop a fully-fledged system that would make this possible is significantly reduced.



FIGURE 4-8: WEBSITE RUNNING ON EROBOT

### IMAGE ACQUISITION

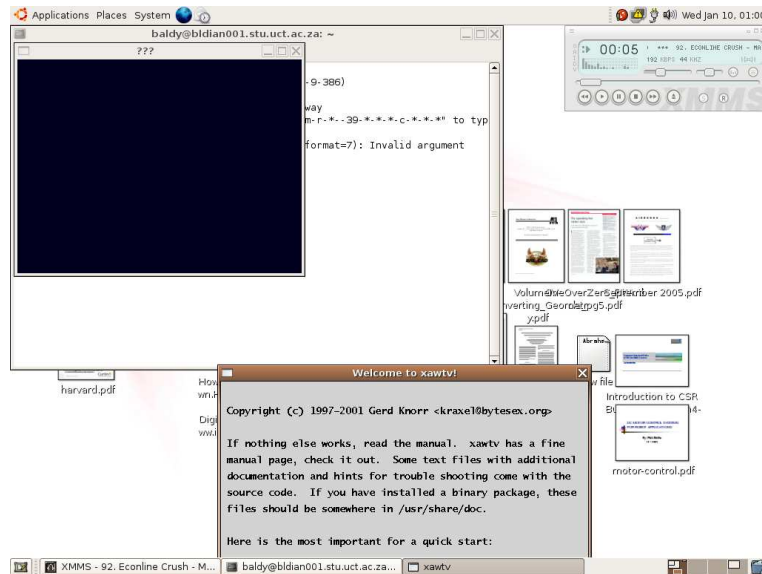


FIGURE 4-9: SCREENSHOT: XAWTV

Storing images from the FireWire camera would be essential in order to correlate the co-ordinate data from the positioning system with the data obtained from the camera in order to build a complete picture of the ship hull. **Xawtv** is an open-source program that allows image capture from webcam devices.



## 4.2 Wireless Communications

Most of the common Linux variants have a package manager utility that enables the installation and upgrading of packages and binaries. Without the package manager, installation of modules becomes a nightmare of manual dependency searches.

In order to allow the robot to download and install required packages, a LAN was set up as shown below:

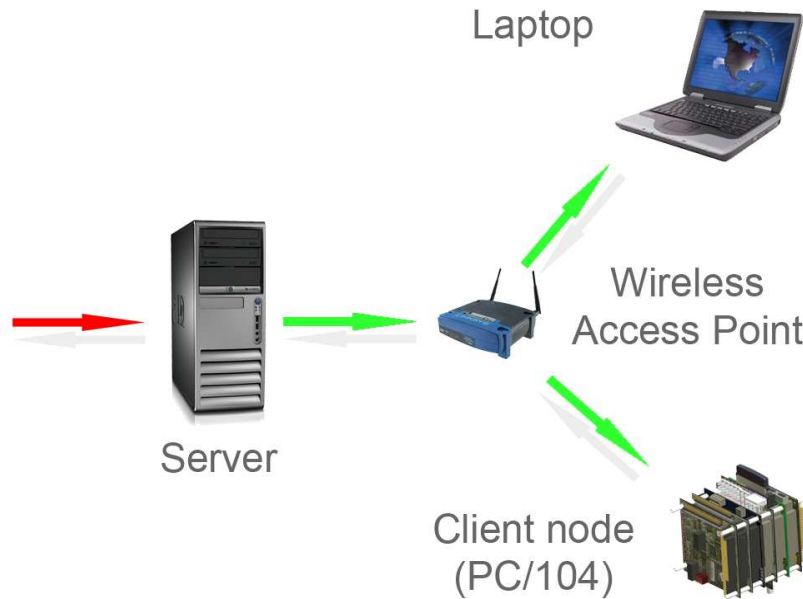


FIGURE 4-10: LAN

In this LAN architecture, the server is free to access the internet. Running on the server is the **Firestarter** daemon, which is an open-source firewall package for Linux. The server then shares its network connection over the wireless network with the LAN clients, which include the robot and a laptop.

One of the major advantages of this setup is that the server acts as a gateway between the LAN clients and the internet, ensuring that malicious network traffic is filtered out. In addition, any number of clients maybe added to the LAN without excessive IT administration issues. Of course with the addition of a client that wishes to access the internet, internet bandwidth for the remaining clients is reduced.

This network type, known as a **Managed** network (as opposed to the point-to-point or **Ad-hoc** network, used in the 1<sup>st</sup> generation prototype) exhibited substantially better client performance in terms of link uptime. Previously, it was not uncommon for the robot to lose the network connection with the laptop several times an hour. In an industry setting this loss would be unacceptable, and would have potentially

far-reaching consequences if the vehicle was operating in a space that was difficult to manually access.

This basic setup, once tested and seen to be viable, was modified to implement a redundant data storage node, as well as the DGPS node.

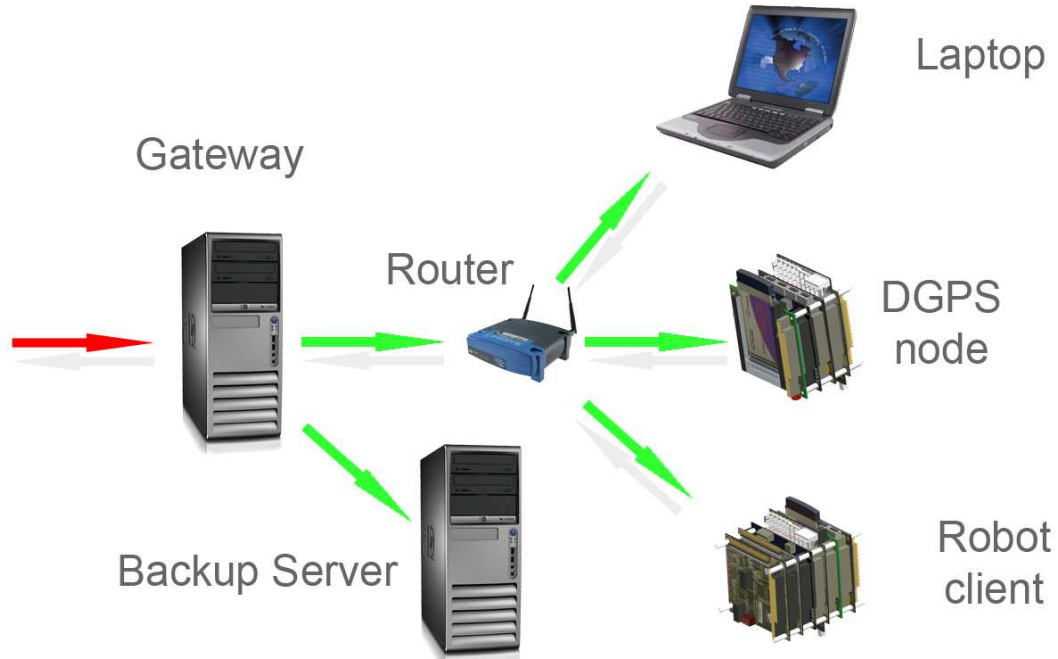


FIGURE 4-11: FULL LAN ARCHITECTURE

The main server mounted the backup-server's disks across a **Network File System (NFS)**. Data stored on the main server was then written to the network disks every 6 hours (there were four file systems) by **cron**, a Linux scheduling daemon.

#### **METHODS & IMPLEMENTATION**

One of the major issues with the initial design was the **latency** or dead-time between when the user moves the joystick, and when the control command is implemented on the platform. At times (in the Windows<sup>®</sup>™ environment), this was in excess of 15 seconds.

As such, one of the challenges of this revision was to reduce (or if possible, eliminate) the latency. One advantage of human-generated control commands (i.e. from a joystick) is that the control implementation only has to be faster than the reaction times of the user. As such a reaction time for the robot (i.e. from when the user inputs a "stop", to when the robot actually stops) must be under half a second.

#### **PROTOCOL SELECTION**

In the first generation robot, Matlab<sup>®</sup> in conjunction with a community-developed tool called **P-net**, was used to control the robot. **P-net** worked by establishing a

**Transmission Control Protocol (TCP)** session between a host and client node. As mentioned previously, this delay (running under Windows<sup>®</sup> 2000) was sometimes in the order of 15 seconds, and never exhibited better performance than 4 seconds. In order to reduce this delay, the decision was made to migrate from higher-level interpreted languages (such as Matlab) to a lower level language such as C++. In addition, a protocol switch was made from TCP to the **User Datagram Protocol (UDP)**. UDP is a connectionless protocol, meaning there is no error checking or handshaking between the host and clients.

<b>TCP</b>	+	Bits 0-3	4-9	10-15	16-31
	0	Source Port			Destination Port
	32	Sequence Number			
	64	Acknowledgment Number			
	96	Data Offset	Reserved	Flags	Window
	128	Checksum			Urgent Pointer
	160	Options (optional)			
	160/192+	Data			

<b>UDP</b>	+	Bits 0 - 15	16 - 31
	0	Source Port	Destination Port
	32	Length	Checksum
	64	Data	

FIGURE 4-12: TCP vs UDP

In **Figure 4-12** above, a comparison of the packet headers is made between the UDP and TCP [35] [36] protocols, with the TCP header at the top. As can be seen from the headers, the TCP protocol requires a lot more *data overhead* per packet, requiring acknowledgement from the recipient to make sure the connection is intact and data integrity will not be compromised.

Conversely, in the UDP packet, all that is required is a destination address and port. This greatly speeds up the packet transmission speed; however it comes at the (potential) sacrifice of data integrity.

However it should be noted that the potential for data loss (or “dropped packets” as they are referred to) is reduced in this network, merely because of the small number of nodes constituting the clients and the corresponding minimal amount of network traffic. As clients nodes are increased, data-integrity checks will have to be implemented on all client-side applications.

#### CODE DIAGRAM

Shown in **Figure 4-13** overleaf is a graphical interpretation of the control flowchart for the system. On the **user side**, an operator makes use of a joystick to send commands across the wireless network to the **client** (in this case eRobot).

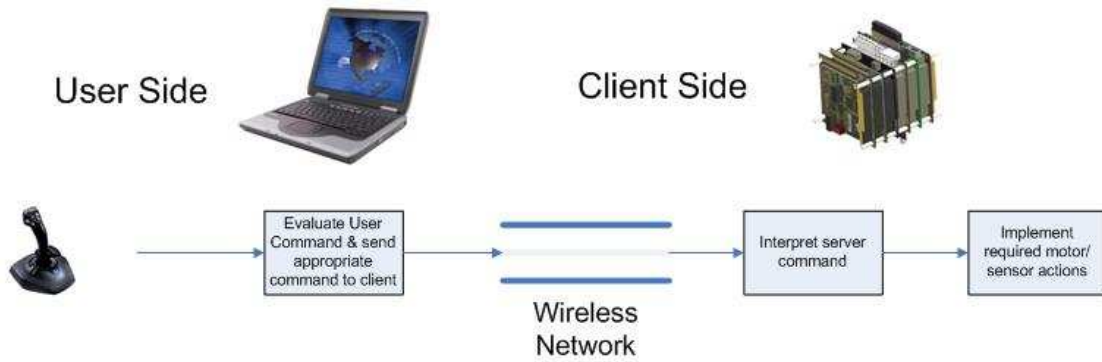


FIGURE 4-13: OVERALL CONTROL

The client is responsible for interpreting the user command and implementing the appropriate commands to the drive units or sensors. This methodology was chosen as it required an absolute minimum of network traffic – a simple command of “forward” could be transmitted from the user side, with all the required implementation (accessing the motor driver and turning both drive motors on) would be implemented by software on the client.

Open-source projects such as the Joystick Wrapper Library [37] and Practical C++ Sockets [38] enabled the author to construct a system that was very responsive to user input and had reaction times in the order of milliseconds.

For a full code listing, please see the documentation in the Appendices and the accompanying DVD.

### 4.3 Global Positioning System (GPS) Locating

The **Global Positioning System (GPS)** has been in widespread civilian use since the mid-nineties, allowing for relatively accurate positioning for outdoor enthusiasts. However, it was only until the removal of **Selective Availability (SA)** in 2000 that GPS became an accurate (within the order of metres) navigational aid.

Officially known as **Navigational Signal Timing and Ranging GPS (NAVSTAR GPS)**, it is operated by the United States Air Force 50<sup>th</sup> Space Wing and consists of 24 space vehicles in medium-earth orbit in six orbital planes [39].

Price and availability of GPS capable units in South Africa have decreased and increased respectively, with several resellers in the Western Cape area having off-the-shelf development boards ready for purchase. For this project the local branch of RF Design was used for all GPS hardware requirements.



FIGURE 4-14: ANTARIS RCB-LJ RECEIVER

Shown in **Figure 4-14** above is the Antaris RCB receiver used in the project. This model is specifically designed for embedded applications, requiring a standard 5V power supply and providing a host of features such as:

Feature	Description
Active Antenna Supervision	Allows for antenna shut-down/start-up for power conservation
DGPS Support	Support for incoming Differential GPS data to facilitate more accurate positioning
Hot/Warm/Cold start	Different switch-on methods:  <b>HOT:</b> Receiver has valid ephemeris, almanac and time, 3.5s Time-to-First Fix ( <b>TTFF</b> )  <b>Warm:</b> Valid ephemeris, valid almanac, not time, 5s TTFF  <b>Cold:</b> Valid almanac, 34s TTFF
NMEA/uBlox message output	Multiple message output formats allow for compatibility with other software/systems

TABLE 2: UBLOX ANTARIS FEATURES

#### DATA OUTPUT

##### NATIONAL MARINE ELECTRONICS ASSOCIATION (NMEA) DATA STRUCTURE

\$	<Address>	{ , <value> }	*<checksum>	<CR><LF>
----	-----------	---------------	-------------	----------

TABLE 3: NMEA DATA STRUCTURE

The NMEA GPS specification is one of the most widely used throughout the world and is supported by most makes and models of GPS units. As such it is useful for interfacing with commercially/publicly available software.

The data consists of a starting \$ sign, the address entry (which describes whether the packet is a positional fix, satellite data, et cetera) and the corresponding value. The penultimate value is a checksum for the packet, with <CR><LF> always terminating the packet. A full description of the protocol can be found on the NMEA website [40].

#### UBLOX DATA STRUCTURE

Synch Char1	Synch Char2	Class	ID	Length	Payload	CK _A	CK _B
----------------	----------------	-------	----	--------	---------	-------	-------

TABLE 4: UBLOX DATA STRUCTURE

uBlox have developed an in-house proprietary system for data display [41]. The uBlox data structure is more descriptive than NMEA 0183 structure; however it is not widely recognised in the open-source community. The first two characters are the synch characters **µ** and **B** (signifying uBlox), followed by the message class which defines the basic message subset and the ID Field which describes the message payload. The length defines the size of the payload, and the 2-byte checksum provides error-checking capability.

#### GPS: ACCURACY

Depending on the receiver (not all makes and models are equal) a conventional GPS signal can be accurate to within several metres. Although this is significantly better than original GPS accuracies before SA was turned off (typically >20m!) it still provides too much of a margin of error for reliable robot positioning. Several techniques are available for the reduction of GPS error, some of which are described below:

#### REAL TIME KINEMATICS (RTK) CORRECTION

By far the most advanced (and hence most difficult to implement) strategy, **Real Time Kinematics** correction is based on the use of carrier phase measurements of GPS satellite signals. RTK finds application in a variety of systems, but when used in conjunction with GPS it is commonly referred to as **Carrier-Phase Enhancement GPS (CPGPS)**. A full explanation of the mechanics of CPGPS is beyond the scope of this thesis, however it is suffice to say it requires sophisticated statistical and analysis techniques with **full access to the raw satellite signal**. However, access to satellite feeds is not provided, so some other method of error correction had to be implemented.

### **DIFFERENTIAL GLOBAL POSITIONING SYSTEM (DGPS)**

Differential **GPS (DGPS)** is a widely used technique that uses a corrected feed from a well-surveyed base station to provide correctional vectors to GPS clients in the area. The principle factor behind DGPS is that the majority of GPS error is generated by the **ionosphere** (the portion of earth's atmosphere reaching upwards from 85 kilometres), and as these errors are usually constant for receivers within the same ionospheric conditions, a large portion of the error can be eliminated.

Of course errors generated from multi-path receptions (where the GPS signal reflects off of local structures i.e. trees, buildings, etc) can not be accounted for, and the correction data will not be applicable to those receivers experiencing differing ionospheric conditions.

#### **DGPS CORRECTION DATA**

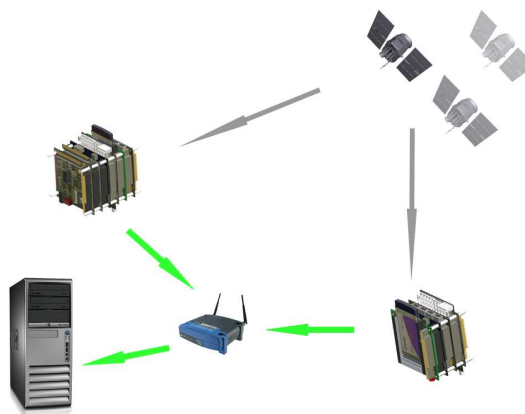


FIGURE 4-15: DGPS SETUP

GPS correction data requires an accurately mapped base-station. In the case of the robot, the base station will be changing all the time, as the mobile portions of the system (i.e. the DGPS node and the robot) are transported from location to location. As such, the method used for the positioning is known as **statistical DGPS**.

In this case, the readings from the robot GPS system are subtracted from the readings given by the stationary base station, giving the difference in position between the base station and the vehicle.

Data from the robot and the station are streamed across the network, meaning any node can have access to the data from every other node. As the data can be streamed on any port, each node can be given an individual port setting to identify itself.



## 4.4 Data Streaming

An important aspect of the robot's performance was its ability to stream data back to the user. Making use of the 802.11g standard allows a maximum transfer rate of 54.0 Mbps. Note that in this case, the standard is defined in megab**its** per second and this translates roughly into 6.75 Megab**ytes** per second. A problem was thus encountered in real-time video streaming. A raw **RGB** (Red, Green and Blue) or YUV (PAL system of analogue video) frame can easily be in excess of 9 Megabytes. This is calculated by frame size (640x480) and multiplied by image "depth" (in the most intensive case, 32-bit colour).

At a standard 30 **frames-per-second (fps)**, this would be 270 Megabytes/second, or 2.2 Gigabits/second. This would overwhelm the network, and therefore to reduce the size of the stream, encoding is used.

However, encoding time introduces a large latency time into the stream due to the compression on the server-side, and decompression on the client side. Using **Video-LAN Client (VLC)** and **Video-LAN Server (VLS)**, popular open-source streaming software, the best latency time achieved was in the order of 3-4 seconds using an MPEG-2 codec.

### NDE PAYLOAD SIMULATION

As there was no dedicated NDE equipment developed for the robot, a standard UniBrain Fire-i FireWire<sup>®</sup> camera was used (**Figure 4-16**, left), the principle being that the camera could record high-definition images of the surface for post-analysis in conjunction with the recorded GPS data.



FIGURE 4-16: UNIBRAIN FIREWIRE CAMERA (LEFT) AND QUICKCAM PRO (RIGHT)

Unfortunately, the Fire-i refused to stream frames to the PC/104 under RedHat 9.0, although it worked on the server box under Ubuntu Badger. This may have been due to RedHat incorrectly generating the **video1394** character device. Therefore, in order to have some form of payload, a QuickCam Pro 4000 (**Figure 4-16**, right) was modified and fitted into the Payload Bay.

## 5. TESTING

### 5.1 Mobility

[For videos of the vehicle in action, please see the accompanying DVD.]



FIGURE 5-1: TESTING OF VEHICLE ON A VERTICAL FERRO-MAGNETIC BOARD

Shown in **Figure 5-1** above is the “testing area” used for the robot. It consisted of a conventional chalkboard bolted onto a wall. While this was probably not completely representative of a real life environment, such as a section of ship hull, it did provide taxing conditions for the robot.

Firstly, the thickness of the board was in the order of 1-2 millimetres. This means that the magnetic flux channelled into the board from the magnets was reduced, providing less adherence capability for the robot. Ship hulls (in good condition) are orders of magnitude thicker, and thus will afford more adherence capability.

Secondly, surface of the chalkboard was coated with an aggregate of chalk and oil/grease. This provided a low-friction surface which sorely tested the traction characteristics of the drive wheels.

#### **VERTICAL ASCENT**

Although the chassis of the robot is relatively light (6 kg’s inclusive of the CM), the weight of the drive units (including wheels) increased the weight to over 8 kg’s. This weight of course had a detrimental effect on the robot’s vertical speed. Despite this, it managed to successfully navigate the entire periphery of the board.

#### **HORIZONTAL TRAVEL**

When not requiring a direct vertical ascent, the robot performed adequately, travelling horizontally (both backwards and forwards) with a minimum of difficulty. This bodes well for its operation in the field, as most scanning would be done in the horizontal plane, with vertical ascents only being performed at the terminal point of the inspection run.

## 5.2 Control

With the implementation of the control code in C++, reaction times of the robot were negligible. Use of UDP streaming across a sparsely-populated network meant that control messages were delivered almost instantaneously, with a typical delivery time being in the order of tens of milliseconds.

This was well within the specified target for the system, and was one aspect of the system that performed well.

## 5.3 Navigation

### GPS POSITIONING

Testing of the platform in the test area practically negated the use of the GPS, as no signal could be obtained. Although the GPS is optimised for use in what is known as “urban canyons” (i.e. the restricted sky-space between tall buildings), it was not capable of attaining a signal in the bottom of a building, which was expected.

### DGPS FEED

Once the server was initialised, it was possible to stream data over the internal network. Initialisation involved positioning the DGPS server so it had access to a substantial portion of the sky, allowing multiple satellite-vehicle signals. Over a period of time, the positional error for the stationary DGPS box tended towards zero. However, this data was of limited use as the robot GPS unit was not capable of receiving a signal.

## 5.4 Data Acquisition

Because of the proximity of the camera to the surface of the chalkboard and the lack of sufficient lighting, images obtained from the device were of poor quality.

## 5.5 Duty Cycle

Model-aircraft Lithium Polymer batteries were used for the **Power Supply Unit**. These units are prolific energy suppliers, capable of supplying 7 Amps (peak current) at 11.1 Volts. Unfortunately, due to their age (the batteries were over 3 years old) 2 battery failures were experienced. Replacement batteries could not be sourced quickly, and therefore full testing of the platform’s operational capabilities was not possible.

---

## 6. CONCLUSIONS & RECOMMENDATIONS

---

*"..[we] decided it was better to come up with a few recommendations, less than ten. No-one takes more than ten recommendations seriously"*

Neil Armstrong, remark made during the *Challenger* Space Shuttle Investigation

Hansen, J.R., 2003, *"First Man: The Life of Neil A Armstrong"*

In conclusion, the base performance of the robot was acceptable. Although the vehicle is not ready for the rigours of an industrial setting, it provided a useful prototype to test the validity of the concept itself as well as other concepts (navigation, networking and so on). The main performance criteria of the system are analysed below and recommendations are made for future development work on the vehicle.

### MECHANICAL DESIGN

Design of the robot in a modular fashion allowed for the simple assembly/disassembly for frequent modifications, and was considered a success. Structurally the robot was sound, and showed no sign of wear at the end of the project.

However, the **weight** of the robot chassis overall meant that the drive units were required to work harder and draw more power from the **PSU** leading to a reduction in the operating time of the robot. In addition, the vehicle failed to ascend at the required speed.

### Recommendation:

#### Aluminium Chassis

Use of an aluminium skeleton would reduce the weight of the robot considerably. HDPE could still be used for panels; however the aluminium frame would be responsible for the rigidity and structural integrity of the vehicle.

#### Redesigned Tail Unit

To compensate for its lack of structural strength, the tail unit was over-designed. In this way it was detrimental to the operation of the vehicle, as the increased weight induced serious performance penalties. A re-design of the unit with aluminium bracing would allow for a lighter assembly.

### ELECTRONICS AND COMPUTING

The use of the **PC/104** stack meant that development time was minimal, as pre-built programs and code could be implemented and tested quickly on the platform, without having to go re-compilation or porting. In this regard the capacity of the PC/104 was not utilised to its full extent, meaning that further behavioural work could be carried out on the platform without the need for any modifications.

If the robot is to be implemented in an industrial setting as is, the excessive computing power of the CM would not be required.

## Recommendation

### Replacement of PC/104

Modern microprocessors such as the ARM9 (used in handhelds and GPS units by PALM® and Garmin® respectively) can support a multitude of peripherals including networking, Bluetooth and high-speed data-transmission protocols such as USB 2.0. Replacement of the PC/104 with a dedicated microcontroller such as the ARM9 would reduce the space, weight and power requirements of the CM.

## NAVIGATION

Use of the networked **GPS system** showed the feasibility of using a Wireless LAN to disseminate positioning information amongst nodes or clients. GPS is an excellent outdoor navigational tool, and with further refinement in its implementation as a navigational aid would be a useful system for accurate positioning of the robot(s), though use of the system in a restricted or “urban-canyon” environment should be avoided as severe signal degradation occurs.

## Recommendation

### Alternative Urban-Canyon Navigational Aid



FIGURE 6-1: ANTARIS SUPERSense® DATA IN A SHOPPING MALL

Use of the standard uBlox Antaris GPS was not feasible for accurate navigation in a sky-restricted environment such as a ship dry-dock. Nearing the end of the project, uBlox released a new version of the Antaris line, the Antaris 4 SuperSense® Indoor GPS. The website describes the unit as providing:

*"...ultra low power consumption, providing reliable indoor coverage for any GPS-endowed application, be it a handheld device or other."* [42]

Replacing the Antaris with the Antaris 4 SuperSense® would allow the vehicle to report accurate positioning information, whilst not requiring any modification to the existing LAN architecture.

As GPS is not well suited for precision altitude measurement, a redundant altitude recording system (such as an ultrasonic pulse-echo system that uses Time-of-Flight calculations to determine height above the ground) should be implemented.

#### **DATA STREAMING**

Use of the QuickCam showed that the idea of visual inspection was possible (which was expected), but it also showed that a redesign would be required if industry-standard pictures are to be obtained.

#### **Recommendation**

##### **Software Upgrade**

Upgrading the entire system to a currently supported Linux version would allow the FireWire bus to be fully utilised. To improve the image quality, super-bright LED's should be embedded around the periphery of the camera to ensure adequate lighting.

##### **Dedicated Streaming System**

Switching to a dedicated streaming protocol such as the **Real-Time Streaming Protocol** would facilitate the streaming of real-time video over the network. This would allow an operator to view the inspection surface as the robot is in motion.

This would mean the vehicle would only have to stop to inspect surfaces that the operator considered to be suspect, speeding up the inspection process.



## REFERENCES

- [1] Stultz, G.R., Bono R.W., Schiefer, M.I., "*Fundamentals of Resonant Acoustic Method NDT*", Advances in Powder Metallurgy and Particulate Materials, 2005 Vol. 3, pp 11-1, 11-11.
- [2] Anderson, T.L., "*Fracture Mechanics: Fundamentals and Applications*", pages 3-5, 1195 CRC Press, Technology & Industrial Arts, 1995.
- [3] "*Phoenix X-Ray: Manufacturers of high-resolution 2D X-ray inspection Systems*", 2006. Accessed on January 9, 2007. Available at:  
[http://www.phoenixxray.com/en/applications/semiconductors\\_electronic\\_components/index.html](http://www.phoenixxray.com/en/applications/semiconductors_electronic_components/index.html)
- [4] "*DNV Exchange: Registry > Knock Nevis*", Det Norske Veritas, Norwegian ship Classification Society. Accessed on January 9, 2007. Available at:  
<https://exchange.dnv.com/exchange/main.aspx?extool=vessel&subview=owner&vesselid=16864>
- [5] Daniel. P, Josse. P, Lefevre. P et al., 2004, "*Forecasting the Prestige Oil Spills*", Proceedings of the 2004 InterSpill Conference and Exhibition.
- [6] Frank, V., March 2005, "*Consequences of the Prestige Sinking for European and International Law*", The International Journal of Marine and Coastal Law Volume 20, no. 1.
- [7] Cohen. M.J, Feb 1995, "*Technological Disasters and Natural Resource Damage Assessment: An Evaluation of the Exxon Valdez Oil Spill*", The Journal of Land Economics, Vol 71 no. 1 , University of Wisconsin Press
- [8] Tscheliesnig. P, Nov 2006 "*Detection of corrosion attack on oil tankers by means of Acoustic Emission (AE)*", Proceedings of the 12<sup>th</sup> Asia-Pacific Conference on NDT, Auckland NZ.
- [9] Constantinis D.A, Richardson A.J, 1994 " *Enhanced Surveys – A cost effective method*", Journal of The Institute of Marine Engineering, Science and Technology, Trans ImarE, Vol. 107, no. 1, pp47-56
- [10] "*History of Robotics*", 2007, Robotics Research Group, University of Texas at Austin. Accessed on January 9, 2007. Available at  
[http://www.robotics.utexas.edu/rrg/learn\\_more/history/](http://www.robotics.utexas.edu/rrg/learn_more/history/)
- [11] Olsen H.O, Vesth L, Jeppesen L, 1998 " *Automated Ultrasonic Examination of Inclined Nozzle Welds Using Robot and 3D Reconstruction*" Proceedings of the 7<sup>th</sup> European Conference on Non-Destructive Testing, Vol. 3, no. 10.



- [12] Slinn, M., 2007, "BONNIE III – *Non-Contact Nuclear Boiler Inspection*". Accessed on January 9, 2007. Available at: <http://www.mslinn.com/sites/mike/OntHydro/>
- [13] Lettich, M.J, 2003, "*Insulation Management and its Value to Industry*" Steam Digest Volume IV, Energy Efficiency and Renewable Energy, U.S Department of Energy. Available at:  
[http://www1.eere.energy.gov/industry/bestpractices/pdfs/steamdigest2003\\_insulation\\_mgmt.pdf](http://www1.eere.energy.gov/industry/bestpractices/pdfs/steamdigest2003_insulation_mgmt.pdf)
- [14] Schmidt, C.W, Jan 2002, "*Petroleum: Possibilities in the Pipeline*" , Journal of Environmental Health Perspectives, Vol. 110 no. 1, The National Institute of Environmental Health Sciences.
- [15] Etkin, D.S, 1999 "*Estimating Cleanup Costs for Oil Spills*", Proceedings of the 1999 International Oil Spill conference no. 168.
- [16] Schempf , H. Chemel, B. Everett, N., June 1995 "*Neptune: above-ground storage tank inspection robot system*", IEEE Robotics & Automation Magazine, Robotics Institute, Carnegie Mellon University.
- [17] Schempf, H., January 31 2006 "*Explorer-II: Wireless Self-Powered Visual and NDE Robotic Inspection System for Live Gas Distribution Mains*", Topical Report for the Department of Energy, National Energy Technology Laboratory, Carnegie Mellon University, The Robotics Institute .
- [18] Abouaf, J., July/August 1998 "*Trial by Fire: teleoperated robot targets Chernobyl*" Journal of Computer Graphics and Applications, Volume 18 Issue 4, pp10-14.
- [19] B.L. Luk, D.S. Cooke, A.A. Collie, N.D. Hower, S. Chen. 2001 "*Intelligent Legged Climbing Service Robot for Remote Inspection and Maintenance in Hazardous Environments*" Proceedings of the 8th IEEE Conference on Mechatronics and Machine Vision in Practice, Hong Kong.
- [20] Arean, P., Muscato, G., Lavorgna, M., Caponetta, R., September 1998 "*New trends in the control of walking robots*", Proceedings of the 1998 IEEE International Conference on Control Applications, Volume 1 pp418-422.
- [21] La Rosa, G., Messina, M., Muscato, G. Sinatra, R., February 2002 "*A low-cost lightweight climbing robot for the inspection of vertical surfaces*", Dipartimento Elettrico Elettronico e Sistemistico, University of Catania, *Mechatronics*, Volume 12 Issue 1.
- [22] "Inspection Robots" 2006, Centre for Energy Systems Research, Tennessee Tech University. Accessed on January 9, 2007. Available at:  
<http://www.cesr.tntech.edu/research/robot/robot.html>

- [23] "*Robotic Crawlers*" 2006, General Electric Inspection Technologies. Accessed on January 9, 2007. Available at: <http://www.geinspectionstechnologies.com/en/products/rvi/rovver/>
- [24] "*Robot Systems*" 2006, MARAT Company, San Buenaventura, California, U.S.A. Accessed on January 9, 2007. Available at: <http://www.maratcompany.com/>
- [25] "*The High Performance All-Terrain Robot: P3-AT*" 2006, MobileRobots Inc. Accessed on January 9, 2007. Available at: <http://www.activrobots.com/ROBOTS/p2at.html>
- [26] Monadjem V., "*Small Explorer Robot for Non-Destructive Testing*", Undergraduate Thesis, Department of Mechanical Engineering, University of Cape Town, 2004
- [27] Baldwin I., "*Sensor Array for Robotic NDT*" Undergraduate Thesis, Department of Mechanical Engineering, University of Cape Town, 2004
- [28] "*Windscreen Wiper Motors and Systems*" 2005, LAP Electrical Limited. Accessed on January 9, 2007. Available at: <http://www.lapelec.co.uk/windscreen14w.htm>
- [29] "*PC/104 Embedded Consortium*" 2008. Accessed on January 9, 2007. Available at: <http://www.pc104.org/>
- [30] "*RTD Embedded Technologies, Inc*" 2006. Accessed on January 9, 2007. Available at: <http://www.rtd.com/>
- [31] "*UCT Linux Enthusiasts Group*" 2007. Accessed on January 9, 2007. Available at: <http://www.leg.uct.ac.za/>
- [32] "*gpsd – a GPS service daemon*" 2007. Accessed on January 9, 2007. Available at: <http://gpsd.berlios.de/index.html>
- [33] "*GpsDrive – GPS Navigation Software for Linux*" 2007. Accessed on January 9, 2007. Available at: <http://www.gpsdrive.cc/>
- [34] "*The Apache Software Foundation*" 2007. Accessed on January 9, 2007. Available at: <http://www.apache.org/>
- [35] "*User Datagram Protocol*" 2007, Wikipedia – The Free Encyclopaedia. Accessed on January 9, 2007. Available at: [http://en.wikipedia.org/wiki/User\\_Datagram\\_Protocol](http://en.wikipedia.org/wiki/User_Datagram_Protocol)
- [36] "*Transmission Control Protocol*" 2007, Wikipedia – The Free Encyclopaedia. Accessed on January 9, 2007. Available at: [http://en.wikipedia.org/wiki/Transmission\\_Control\\_Protocol](http://en.wikipedia.org/wiki/Transmission_Control_Protocol)
- [37] "*libjsw – Joystick Wrapper Library*" 2006. Accessed on January 9, 2007. Available at: <http://wolfpack.twu.net/libjsw/>
- [38] Donahoo, J. 2007 "*Practical C++ Sockets*". Accessed on January 9, 2007. Available at: <http://cs.baylor.edu/~donahoo/practical/CSockets/practical/>

- [39] "NAVSTAR Global Positioning System Joint Program Office" 2006. Accessed on January 9, 2007. Available at: <http://gps.losangeles.af.mil/>
- [40] "The National Marine Electronics Agency" 2007. Accessed on January 9, 2007. Available at: <http://www.nmea.org/>
- [41] "u-center Mobile" 2007. Accessed on January 9, 2007. Available at: [http://www.u-blox.com/products/u\\_center\\_mobile.html](http://www.u-blox.com/products/u_center_mobile.html)
- [42] "SuperSense<sup>®</sup> Indoor GPS" 2007. Accessed on January 9, 2007. Available at: <http://www.u-blox.com/technology/supersense.html>
- [43] "Glossary of Terms", The Corrosion Source Handbook, 2002. Accessed on January 9 2007. Available at: [http://www.corrosionsource.com/handbook/glossary/f\\_glos.htm](http://www.corrosionsource.com/handbook/glossary/f_glos.htm)
- [44] "Neodymium Magnet" 2007, Wikipedia – The Free Encyclopaedia. Accessed on January 9, 2007. Available at: [http://en.wikipedia.org/wiki/Neodymium\\_magnet](http://en.wikipedia.org/wiki/Neodymium_magnet)
- [45] 2007, "Motor Control Bridges > LMD18200", National Semiconductor. Accessed on January 15, 2007. Available at: <http://www.national.com/pf/LM/LMD18200.html>

---

## GLOSSARY & ACRONYMS

---

### GLOSSARY

Eagle/CAD - An open-source/commercial Electrical Computer Aided Design package

Fracture mechanics – “A quantitative analysis for evaluating structural behaviour in terms of applied stress, crack length, and specimen or machine component geometry” [43]

G-Code – A common programming language [of which many versions exist] for **Computer Numerically Controlled (CNC) Machines**

H-Bridge – An Integrated Circuit or collection of discrete components that allows a Direct Current motor to be run forwards or backwards.

Jockey Wheel – A non-driven wheel, included for balance or load sharing

Neodymium – A rare earth metal that, in conjunction with Iron and Boron, constitute the elements of powerful rare-earth NIB magnets.[44]

PC/104 – A stackable computing form factor.

Pro/Engineer – A parametric 3D **Computer Aided Design (CAD)** Package.

Pro/MANUFACTURE – A prismatic machining extension to Pro/ENGINEER.

Ultrasonic inspection – A method of flaw-detection that makes use of the Time-of-Flight of ultrasonic waves through metals to determine their thickness and potential flaw locations.

WiFi – Wireless Fidelity, a widely used term for high-frequency **Wireless Local Area Networks (WLAN's)**

### ACRONYMS

CNC – Computer Numerical Control

CM – Computing Module

DGPS – Differential GPS

EU – European Union

EM – Electronics Module

FEA – Finite Element Analysis

GPS – Global Positioning System

HDPE – High Density Polyethylene

IC – Integrated Chip

ISA – Industry Standard Architecture

I/O – Input/Output

LAN – Local Area Network

NDE – Non Destructive Evaluation

NMEA – National Marine Electronics Association

PCB – Printed Circuit Board

PCI – Peripheral Component Interconnect

PCMCIA – Personal Computer Memory Card International Association

PSU – Power Supply Unit

PWM – Pulse Width Modulation

TU – Tail Unit

XML – eXtensible Mark-up Language

---

## **BIBLIOGRAPHY**

---

Negus, C., 2005 "*Linux Bible, 2005 Edition*", Wiley Publishing, Inc.

Sobell, M., 2006 "*A Practical Guide to Red Hat Linux*", Third Edition, Prentice Hall

Scherz, P., 2000 "*Practical Electronics for Inventors*" McGraw-Hill

Horowitz, P., Hill, W., 2002 "*The Art of Electronics*" Second Edition, Cambridge University Press

---

## **APPENDIX A: LITERATURE REVIEW**

---





---

## **APPENDIX B: DESIGN AND MANUFACTURE**

---





An Industrial NDE robot

---

## **APPENDIX C: COMPUTER SYSTEM SETUP & CODE**

---